Nanocapsules containing Saussurea lappa essential oil: Formulation, characterization, antidiabetic, anti-cholinesterase and anti-inflammatory potentials

Narimane Lammari, Tanguy Demautis, Ouahida Louaer, Abdeslam Hassen Meniai, Hervé Casabianca, Chawki Bensouici, Gilles Devouassoux, Hatem Fessi, Abderrazzak Bentaher, Abdelhamid Elaïssari

Nanocapsules Containing *Saussurea lappa* Essential Oil: Formulation, Characterization, Antidiabetic, Anti-Cholinesterase and Anti-Inflammatory Potentials.

Narimane Lammari [a,b], Tanguy Demautis [c], Ouahida Louaer [b], Abdeslam Hassen Meniai [b], Herve Casabianca [d], Chawki Bensouici [e], Gilles Devouassoux [c], Hatem Fessi [a], Abderrazzak Bentaher [c], Abdelhamid Elaissari [a,*]

[a] Univ Lyon, Université Claude Bernard Lyon-1, CNRS, LAGEPP UMR 5007, F-69622 Lyon, France

[b] Environmental Process Engineering Laboratory, University Constantine 3, Salah Boubnider, 25000 Constantine, Algeria.

[c] Inflammation and Immunity of the Respiratory Epithelium - EA7426 (PI3) - South Medical University Hospital - Lyon 1 Claude Bernard University, Pierre-Bénite, France

[d] CNRS, Central Service of Analysis, Institute for Analytical Sciences, Villeurbanne.

[e] Centre de Recherche en Biotechnologie (CRBt), 25000 Constantine, Algeria.

*** Corresponding author:** Abdelhamid Elaissari; abdelhamid.elaissari@univ-lyon1.fr

Abstract

Plant-based remedies have been widely used for the management of variable diseases due to their safety and less side effects. In the present study, we investigated *Saussurea lappa* CB. Clarke. (SL) given its largely reported medicinal effects. Specifically, our objective was to provide an insight into a new polymethyl methacrylate based nanocapsules as carriers of SL essential oil and characterize their biologic functions. The nanoparticles were prepared by nanoprecipitation technique, characterized and analyzed for their cytotoxicity, anti-inflammatory, anti-Alzheimer and antidiabetic effects. The results revealed that the developed nanoparticles had a diameter around 145 nm, a polydispersity index of 0.18 and a zeta potential equal to +45 mV and they did not show any cytotoxicity at 25 $\mu g \cdot mL^{-1}$. The results also showed an anti-inflammatory activity (reduction in metalloprotease MMP-9 enzyme activity and RNA expression of inflammatory cytokines: TNF-α, GM-CSF and IL1β), a high anti-Alzheimer's effect (IC50 around 25.0 and 14.9 $\mu g \cdot mL^{-1}$ against acetylcholinesterase and butyrylcholinesterase, respectively), and a strong antidiabetic effect (IC50 were equal to 22.9 and 75.8 $\mu g \cdot mL^{-1}$ against α-amylase and α-glucosidase, respectively). Further studies are required including the *in vivo* studies (e.g., preclinical), the pharmacokinetic properties, the bioavailability and the underlying associated metabolic pathways.

Keywords

Saussurea lappa, essential oil, nanoparticles, antidiabetic, anti-Alzheimer, anti-inflammatory.

1. Introduction

Nature is an inexhaustible source of molecular varieties with a great therapeutic potential, representing nowadays a valuable pool for the identification of novel drug leads (Calixto, 2019; Koparde et al., 2019). In the past decades, pharmaceutical industry has shifted its main focus toward the synthetic products due to their easy quality control, production cost and time effectiveness (David et al., 2015). However, their cost, safety and efficiency remained always questionable, resulting in the dependence on the plant-based drug discovery by more than 80% of the total population in developed countries (Veeresham, 2012). Since a long time plant-based drug discovery had been the basis in the medical management of a great number of known diseases and body malfunction (Atanasov et al., 2015). *Saussurea lappa* CB. Clarke. known as costus, belongs to the Asteraceae family and is well known for its enormous medicinal effects. Ethnopharmacological surveys have pointed that the roots and leaves of the plant are used in the traditional treatment of several diseases like throat infection, cough, asthma, leprosy, tuberculosis, malaria, inflammation, convulsion, helminthic infestation and rheumatism (Gautam and Asrani, 2018; Kaur et al., 2019; Madhuri et al., 2012; Singh et al., 2017; Zahara et al., 2014). *Saussurea lappa* (SL) is considered as a rich source of triterpenoids, flavonoids, steroids and sesquiterpene lactones (Singh et al., 2017), and is reported to have several biological potentials including antimicrobial (Abdelwahab et al., 2019), larvicide (Liu et al., 2012), antioxidant (Sadik et al., 2017), antihepatotoxic (Ansari et al., 2018), anti-inflammatory (Tag et al., 2016), anticancerous (Tian et al., 2017), antiulcerous (Sutar et al., 2011), anticonvulsant (Dhar et al., 2016) and antidiabetic activities (Raafat et al., 2019). A literature survey revealed that most of the studies dealt with the investigation of

the biological effects of the SL extracts, which were obtained by using the conventional organic solvent extraction processes.

Simultaneously with the emergence of plant-based drug formulations, the pharmaceutical field has known during the last era a steady growth in investment in nanotechnology in order to improve existing treatments and develop novel therapies (Matteucci et al., 2018). Polymeric nanoparticles (NP) have been proposed as a novel approach to overcome difficulties encountered in traditional drug delivery such as poor aqueous solubility, low bioavailability, poor stability and bitter taste (Giaretta et al., 2019; Ma and Williams, 2018; Umerska et al., 2018). Sonaje et al. (2010) noticed an enhanced intestinal absorption of insulin, a prolonged reduction in blood glucose levels and an increased bioavailability upon insulin encapsulation in chitosan/ poly(*γ*-glutamic acid) based NP. Moreover, Huh et al. (2005) demonstrated that encapsulation of paclitaxel upsurge dramatically its water solubility by a factor of 1000 and ensure its long-term stability. Additionally, these nanocarriers (nanospheres or nanocapsules) may provide preferential accumulation of bioactive agents at a specific tissue or cell (Lombardo et al., 2019).

Poly (ethyl acrylate-co-methyl methacrylate-co-trimethylammoniethyl methacrylate chloride) (PMMA), a synthetic polymer known as Eudragit® RS100, was widely used for developing polymeric NP due to its crucial features including biocompatibility, permeability, non-toxicity, non-irritancy and controlled drug release profile (Hani et al., 2011). In addition, PMMA was known for its mucoadhesive property. For instance, an electrostatic interaction would be expected between its ammonium groups

and negatively charged chemical groups of bioactive agent or target tissue surface (i.e. mucin) resulting in boosting cellular uptake (Dillen et al., 2008; Tayel et al., 2013).

The last decade had seen the integration of nanotechnology and herbal medicine to overcome the limitations of using herbal formulations in a scientific way in the aim to promote an efficient therapeutic action (Pattabhiramaiah et al., 2020). The expected benefits from the encapsulation of plant-based products included an enhanced aqueous solubility and bioavailability, a better protection from the environment (pH, temperature, humidity and oxygen) and a persistent delivery (Bilia et al., 2014). Several studies have been dedicated to the encapsulation of plant derived-metabolites such as essential oil (EO) (Chifiriuc et al., 2017; El-Asbahani et al., 2015; Froiio et al., 2019; Herculano et al., 2015; Jummes et al., 2020; Partheniadis et al., 2020; Pina-Barrera et al., 2019; Timbe et al., 2020), vegetable oils (Contri et al., 2013, 2016; Lammari et al., 2020a; Sousa et al., 2013), plants extracts (Azeez et al., 2020; Ma et al., 2018; Mughees et al., 2020; Servat-Medina et al., 2015), etc. However, to the best of our knowledge, neither the extract nor the EO of costus roots have been previously encapsulated in polymeric nanoparticles.

In this study, we report for the first time, the encapsulation of SL-EO in PMMA based-NP and the investigation of their cytotoxicity, anti-inflammatory, anti-Alzheimer and antidiabetic potentials of such formulation. First and contrary to the majority of previously reported studies to extract SL-EO, an innovative and environmentally friendly technique (supercritical CO_2 extraction process) was used to obtain an extract free of any traces of organic solvents. Then, a gas chromatography analysis coupled to mass spectroscopy (GC-MS) was carried out in order to characterize the obtained SL-EO before its encapsulation in PMMA-NP. The obtained particles were then characterized by

dynamic light scattering, Fourier transform infrared spectroscopy (FTIR) and transmission electron microscopy. Finally, *in vitro* cytotoxicity, anti-Alzheimer, antidiabetic and anti-inflammatory activities were investigated for SL-EO in its free and encapsulated form.

2. Material and methods

2.1. Plant material

The dried roots of Indian *Saussurea lappa* CB. Clarke. were purchased from herb store (Bordj Bou Arreridj, Algeria). The roots were washed with water, air dried, ground to an approximate size of 0.3 mm and stored in air-tight bottles ready for further analysis.

2.2. Chemical reagents

Eudragit RS®100 was purchased from EVONIK (EVONIK, Germany). Carbon dioxide (99.5%) was supplied by SIDAL SPA Air liquid, Algiers, Algeria. Acarbose (≥95%), 4-nitrophenyl-α-D-glucopyranoside (≥99%), starch powder, acetylthiocholine iodide, S-butyrylthiocholine iodide, 5,5′-dithiobis(2-nitrobenzoic) acid (DTNB), galantamine, *Aspergillus oryzae*-derived α-amylase, *Saccharomyces cerevisiae*-derived α-glucosidase (Type I, ≥10 units/mg protein), electric eel-derived acetylcholinesterase (AChE, Type-VI-S, EC 3.1.1.7, 827.84 U/mg, Sigma) and horse serum-derived butyrylcholinesterase (BChE, EC 3.1.1.8, 7.8 U/mg, Sigma) were all obtained from Sigma Chemical Co. (Sigma-Aldrich GmbH, Sternheim, Germany). Potassium iodide was obtained from Biochem Chemopharma. Deionized water from Milli-Q system was used in all experiments. All other chemicals and solvents were of analytical grade.

2.3. Extraction of essential oil

The dried powder (80 g) of SL was subjected to the supercritical carbon dioxide extraction using a dynamic pilot-plant (Separex 4343, type SF2) supplied by Separex

(Champigneulles, France). The operating extraction parameters were as follow: dynamic extraction time: 180 min; CO_2 flow rate: 50 g/min; CO_2 pressure: 100 bar; extraction temperature: 40°C and separation temperature: 30°C (**Fig.1**). The oil yield value was determined around 23%.

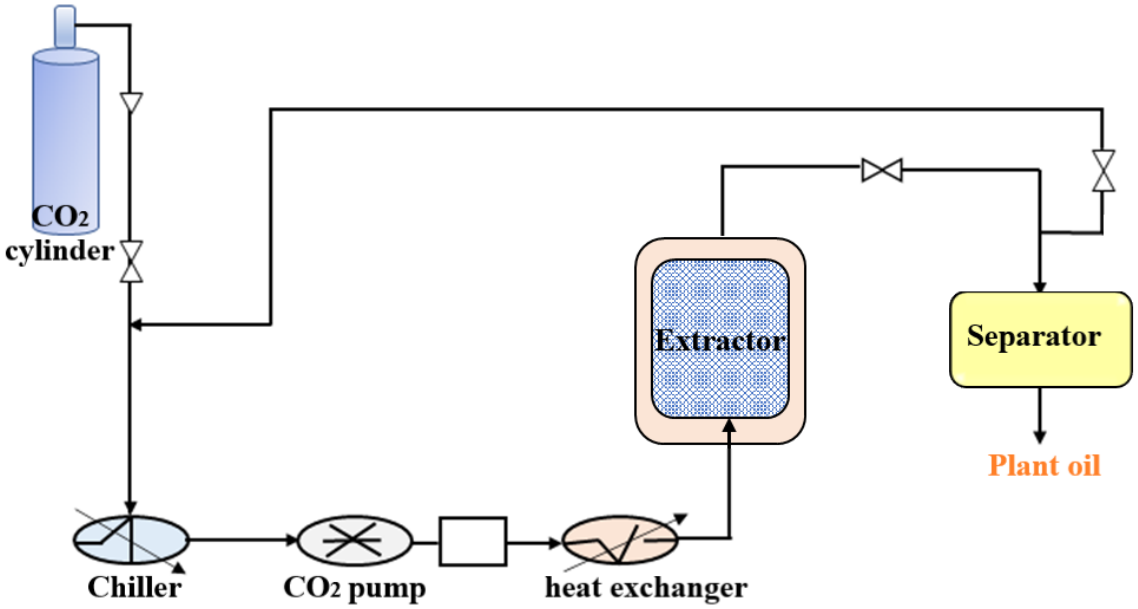

Fig.1. Supercritical carbon dioxide extraction pilot.

2.4. Gas Chromatography analysis of *Saussurea lappa* EO

Analysis of SL-EO was performed at the Institut des Sciences analytiques (ISA), CNRS, at Villeurbanne, France, using two GC systems, equipped with two kinds of capillary columns:

2.4.1. Gas Chromatography – Flame Ionization Detector (GC-FID)

The analysis was carried out on an Agilent 6890N apparatus equipped with a split / splitless injection and a FID detector. SL-EO (1 µL volume) was firstly injected in split mode (1/60) to an INNOWAX column (60m × 0.32 mm, 0.50-µm film thickness) under a

constant flow (1.3 mL/min rate) of helium used as gas carrier. The initial temperature of the column was maintained constant at 60°C for 2 min and then programmed to 245°C at a rate of 2 °C/min and then held isothermally for 30 min. A second injection was conducted on a HP-1 (Agilent) column (50m × 0.32 mm, 0.50-µm film thickness) with a temperature program as follow: 8 min at 80 °C, increased to 220 °C at a rate of 2 °C/min and then increased to 310 °C at 10 °C/min and finally held isothermally 20 min at 310 °C. Helium was used as the carrier gas at a constant pressure (13psi). In both cases, the analyses were performed with injector and detector temperatures maintained at 250 °C.

2.4.2. Gas Chromatography-Mass Spectrometry (GC-MS)

The EO components were identified by mass spectrometry 6890N gas chromatography coupled to Agilent 5973N mass selective detector. SL-EO (1 µL volume) was injected in a split mode (1/60) at 250℃ to an HP-5MS capillary column (0.25 mm × 30 m, 0.25-µm film thickness). The operating conditions were as follows: the GC temperature program was held at 60℃ for 2 min, then increased at 3℃/min from 60℃ to 250℃ , held at 250℃ for 2 min, increased to 325℃ at 10℃ /min, and then held isothermally for 15min; helium flow rate was maintained at 1.0 mL/min; the MS energy ionization was set at 70 eV; electron ionization mass spectra were acquired in scan mode over the mass ranged 35–350 Daltons.

5.4.3. Identification of *Saussurea lappa* EO components

Relative percentages of SL-EO components were determined basing on their GC peak areas without using correction factors. The retention indices were determined by linear interpolation in relation to a homologous series of n-alkanes (C_5–C_{30}) injected on the two capillary columns under the same operating conditions with that of literature data and

those of the add-in-house database available in the ISA laboratory. Further identification was made by computer matching with two commercial mass spectral libraries (NIST data gateway database 2005 and Wiley).

2.5. Preparation of PMMA loaded nanoparticles

PMMA-NP were prepared by means of the nanoprecipitation technique (Fessi et al., 1989) using a protocol that was already described and studied systematically throughout the blank nanoparticles preparation (Lammari et al., 2020a) and according to which 220mg of PMMA was dissolved in 15mL of ethanol and then mixed with 120mg SL-EO. Consecutively the prepared organic phase was added carefully and very slowly to the aqueous phase consisting of 30 mL water at ambient temperature and under moderate magnetic stirring. The evaporation of the organic solvent was performed subsequently using Buchi Rotavapor R-124®. For blank nanoparticles, the same step was repeated without EO.

2.6. Characterization of PMMA loaded nanoparticles

2.6.1. Size distribution, polydispersity index, and zeta potential

In order to determine the average diameter, polydispersity index and zeta (ζ)-potential, the aqueous suspension of PMMA-NP was subjected to an analysis by dynamic light scattering (DLS) technique using a Zetasizer Nano ZS200 (Malvern Instruments, UK). Previous to each size measurement, nanoparticles were diluted in 1 mL of distilled water. While measuring the ζ- potential of prepared nanoparticles, a colloidal dispersion was made in 1mM NaCl solution. All the measurements were performed in triplicate at ambient temperature and pH around 6.5 and the results were expressed as means and standard deviations.

2.6.2. Transmission electron microscopy

The morphology of the NP was investigated immediately after preparation, using a Philips CM120 microscope operated at 120 kV, at the "Centre Technologique des Microstructures" (CTμ) at the University of Lyon (Villeurbanne, France). Drops of the nanoparticle suspensions were placed on microscope grid (copper support covered with carbon) and the grids were analyzed after being allowed to dry by evaporation.

2.6.3. Fourier transform infrared spectroscopy

The infrared spectra of PMMA, un-encapsulated SL-EO and SL-EO loaded-NP were investigated using an FTIR spectrometer (Thermo Scientific Technologies FTIR spectrometer with IR MONIC Solution software). In this study, the oil loaded NP were freeze dried then analyzed; while, no initial preparation was taken place for SL-EO and PMMA. All spectra were recorded from 400 to 4000 cm^{-1} wavenumber range. Prior to each acquisition, blank background had been adjusted.

2.7. Stability study of *Saussurea lappa* EO-loaded PMMA nanoparticles

In order to assess the colloidal stability, the obtained EO-loaded NP were stored for a period of one month at 4, 25 and 40°C. Nanoparticles physical stability was assessed via particle size and ζ-potential measurements which were carried out after each 10 days.

2.8. Cell and culture conditions

Human adenocarcinomic alveolar epithelial cells (A549), supplied by American Type Culture Collection LGC Standard, Molsheim, France, were cultured in DMEM/F-12 (Gibco®, Thermo Fisher Scientific, Waltham, MA, USA) enriched with 10% FBS (Gemini® Bio-Products, West Sacremento, CA) and 1% penicillin/streptomycin (Life Technologies®, Grand Island, USA). Cells were grown in a humidified 5% CO_2 incubator at 37°C.

2.9. Cytotoxicity test

At 80% of confluence, A549 cells were treated with SL-EO-solution (SL-EO dissolved in dimethylsulfoxide (DMSO)), blank NP (non-loaded) and SL-EO loaded-NP formulations using different concentrations (12.5, 25, 50, 75, 100 and 200 µg/mL of oil content) for 24 h. After treatment, culture supernatants were harvested and released LDH was measured using Pierce LDH cytotoxicity assay kit (Thermo Fisher Scientific, Waltham, MA, USA) according to the manufacturer's protocol.

2.10. Microscopy

After cell treatments, changes in morphology of A549 cells were observed through optical microscope after fixation and coloration with Kwik-Diff kit (Thermo Fisher Scientific, Waltham, MA, USA).

2.11. Anti-inflammatory activity

A549 cells were treated, when they reach 80% of confluence, with SL-EO loaded-NP at the concentration of 25 µg/mL of oil content 1 h prior to lipopolysaccharides (LPS) (1 µg/mL) stimulation. After 1 h post LPS exposure, cells were lysed and processed for total RNA extraction and mRNA expression analysis.

2.11.1. Total RNA extraction

Total cellular RNA was isolated using TRI Reagent (Sigma) according to manufacturer instructions. Quality and quantity RNA were controlled with a Nanodrop spectrophotometer (ThermoScientific).

2.11.2. Real-Time PCR

The expression of mRNA was determined using Taqman quantitative Real-Time PCR on cDNA acquired from Reverse Transcriptase-PCR using Superscript TM IV

(Thermo Fischer Scientific), following manufacturer specifications. Product was amplified with commercially available Taqman primers and Taqman Mastermix (Life Technologies) on AriaMx Real-time PCR system. The product reference for Taqman primers were the following: hTBP (Hs99999910_m1), hCSF2 (Hs00929873_m1), hTNFα (Hs00174128_m1) and hIL1β (Hs 01555410_m1). Real-Time PCR data was analyzed using the comparative Ct (ΔΔCT) method.

2.11.3. Gelatin zymography

Gelatin zymography to detect active proteases namely metalloproteases (MMP) was performed using cell culture supernatants of untreated and treated cells. Briefly, the samples were subjected to sodium dodecyl sulphate-poly acrylamide gel electrophoresis (SDS-PAGE) on 10% polyacrylamide containing 0.1% SDS and 1.5 mg/mL gelatin under non-reducing conditions without prior boiling. After electrophoresis, gels were washed in 2% Triton X-100 for 1 hour to remove SDS, and subsequently immersed in a mixture containing Tris-HCl (50 mM/L) (pH 7.6), $CaCl_2$ (5 mM/L) and $ZnCl_2$ (0.5µM/L) for 24 hours at 37°C. The gels were then stained (5g Coomassie Brilliant Blue, 200 mL methanol, 50 mL acetic acid, 500 mL distilled deionized water) for 10 minutes at room temperature on a rocker and then destained in 20% methanol /10% acetic acid. Enzymatic activities were detected as clear bands of gelatin lysis against the blue background. Gels were scanned using ChemidocXRS BIORAD and analyzed with FIJI software. Densitometric analysis was performed on captured images, using ImageJ software.

2.12. *In vitro* cholinesterase activity assay

Cholinesterase activities of SL-EO loaded-NP, un-encapsulated oil and free NP were evaluated *in vitro* against Acetyl and Butyryl cholinesterase enzymes based on

Ellman's method (Ellman et al., 1961) using a 96-well microplate reader, PerkinElmer Multimode Plate Reader EnSpire (National Center of biotechnology Research, Constantine, Algeria). Different concentrations of sample solution (10 µL) were mixed and incubated for 15 min at 25 °C with 150 µL of sodium phosphate buffer (100 mM, pH 8.0) and 20 µL of acetylcholinesterase or butyrylcholinesterase solution. Then, 10 µL of 0.5mM DTNB was added along with 10 µL of acetylthiocholine iodide or butyrylthiocholine iodide. Galantamine hydrobromide was used as positive control. The absorbance was read at 412 nm utilizing a 96-well microplate reader. the IC50 (the concentration providing 50% enzyme inhibition) was calculated by plotting inhibition percentage against sample concentration.

2.13. *In vitro* alpha-amylase and alpha-glucosidase activity assay

The study of the antidiabetic activity of SL-EO loaded-NP, un-encapsulated oil and free NP was evaluated *in vitro* through the inhibition of two key enzymes (α-amylase and α-glucosidase) based on quantitative colorimetric assays using a 96-well microplate reader, PerkinElmer Multimode Plate Reader EnSpire (National Center of biotechnology Research, Constantine, Algeria).

2.13.1. Alpha amylase activity

Alpha amylase inhibitory activity was investigated using Caraway-Somogyi iodine/potassium iodide method as previously described with slight modifications (Yang et al., 2012). Different concentrations of sample (25 µL) were mixed with α-amylase solution (50 µL) and incubated at 37 °C for 10 min. Then, the reaction was started by adding starch solution (50 µL, 0.1%). Similarly, a blank was prepared by adding sample solution to all reaction reagents without enzyme solution. After incubation (10min at

37°C), the reaction was stopped by adding 25 µL HCl (1 M) and 100 µL iodine-potassium iodide solution. Acarbose was used as standard. The sample and blank absorbances were read at 630 nm by micro plate reader and the IC50 of all the formulations was calculated.

2.13.2. Alpha glucosidase activity

Alpha glucosidase inhibitory activity was measured using a method previously described with slight modifications (Vadivelan et al., 2019). In 96-well microplate, different concentration of sample solution (50 µL) were mixed with 100 µL of 0.1 M phosphate buffer (pH 6.9) containing α-glucosidase solution and incubated at 37 °C for 15 min. Next, 50 µL of 5 mM *p*-nitrophenyl-α-D-glucopyranoside solution in 0.1 M phosphate buffer (pH 6.9) was added. After incubation (5 min at 37 °C), the sample and blank absorbances were read at 405 nm and the IC50 of all the formulations was determined. Acarbose was used as standard.

2.14. Statistical analysis

The data values are expressed as mean ± standard deviation (SD). The statistical significance of the differences between samples was determined using XLSTAT software with one-way analysis of variance (ANOVA) with Tukey post-test; $p < 0.05$ was selected such as criterion for significant differences.

3. Results and discussion

3.1. Gas chromatography analysis

To illustrate the chemical composition of SL-EO, two complementary methods were used: GC-FID and GC-MS. Two different kinds of capillary columns were used as well: the polar HP-Innowax and the apolar HP-1 in the aim of facilitating the separation and resolving the problem of co-elution of some compounds. The relative percentages of

SL-EO components were depicted in **Table 1**. A total of 21 components of the EO were identified, accounting for 82.75 % of the total oil. The principal compounds in SL-EO were dehydrocostus lactone as the major compound (55.39 %) followed by costunolide (8.87%), dehydrosaussurea lactone (6.55%) and aplotaxene (4.73%). Oxygenated sesquiterpenes represented 13 out of the 21 compounds, corresponding to 75.92% of the whole EO, while 8 out of the 21 constituents were hydrocarbons sesquiterpenes, corresponding to 5.94% of the crude EO. The chemical composition of EO was in a good agreement with that reported in previous works (Chen et al., 2011; Liu et al., 2012; Zahara et al., 2014). Chen et al. reported that the EO extracted form costus roots collected from seven producing areas (provinces) all contained the two main components, dehydrocostus lactone (ranging from 16.30 to 25.36%) and costunolide (ranging from 4.28 to 8.32%) (Chen et al., 2011). Variation in EO composition may be ascribed to climatic and seasonal factors, harvest time and local as well as storage duration of medicinal plants. Dehydrocostus lactone and costunolide, are sesquiterpenes lactones, very known for their anticancer (Lin et al., 2015; Peng et al., 2017), anti-inflammatory (Park et al., 2014; Scarponi et al., 2014), gastro-protective (Zheng et al., 2016), anti-osteoclastogenic (Cheon et al., 2014; Li et al., 2019), antibacterial (Negi et al., 2014) and larvicidal (Liu et al., 2012) activities. Dehydrosaussurea lactone (8.87%) is very similar structurally to costunolide and has been previously shown to exhibit an anticancer activity by inducing cell cycle arrest against various cell lines (Chang et al., 2010), while, aplotaxene has been recently regarded as a bioactive agent in the treatment of autoimmune and inflammatory diseases due to its immunosuppressive effect on T cells (Na et al., 2013).

Other compounds of significant medicinal and biological interests were identified in trace amounts in SL-EO (**Table 1**) and these include: β-eudesmol, a sesquiterpene, which was recently shown as an effective inhibitor of SARS-CoV-2 main protease (Aanouz et al., 2020), caryophyllene oxide as an analgesic and anti-inflammatory agent (Chavan et al., 2010), β-ionone as antioxidant and anticancer agent (Asokkumar et al., 2012) and α-humulene which was found as effective bioactive agent to inhibit drug-metabolizing enzymes in human liver (Nguyen et al., 2017).

Table 1. *Saussurea lappa* essential oil chemical composition as determined by gas chromatography - flame ionization detector (GC - FID) and gas chromatography - mass spectrometry (GC-MS).

No	Component	Formula	RI-HP-1	RI-WAX	Content (%)
1	Beta elemene	$C_{15}H_{24}$	1388	1808	0.288
2	Dihydroionone	$C_{13}H_{22}O$	1396	-	0.088
3	Alpha ionone	$C_{13}H_{20}O$	1406	1876	0.147
4	Trans Beta Caryophyllene	$C_{15}H_{24}$	1419	1628	0.288
5	Neryl acetone	$C_{13}H_{22}O$	1428	-	0.029
6	Alpha humulene	$C_{15}H_{24}$	1452	1704	0.033
7	Beta ionone	$C_{13}H_{20}O$	1464	1946	0.093
8	Alpha + Gamma curcumene	$C_{15}H_{22}$ /$C_{15}H_{24}$	1471	1801/1719	0.06
9	Pentadecene-1	$C_{15}H_{30}$	1474	1539	0.06
10	Beta selinene	$C_{15}H_{24}$	1482	1750	0.308
11	Alpha selinene	$C_{15}H_{24}$	1493	1758	0.17
12	Alpha elemol	$C_{15}H_{26}O$	1534	2108	0.085
13	Elema- 1,3,11(13)-Trien-12-al	$C_{15}H_{22}O$	1555	-	0.206
14	Oxyde Caryophyllene	$C_{15}H_{24}O$	1570	2024	0.291
15	Beta Eudesmol	$C_{15}H_{26}O$	1636	2268	1.256
16	Aplotaxene	$C_{17}H_{28}$	1660	2623	4.734
17	Beta costol	$C_{15}H_{24}O$	1748	2532	1.865
18	Alpha costol	$C_{15}H_{24}O$	1754	2607	1.034
19	Dehydrosaussurea lactone	$C_{15}H_{20}O_2$	1861	-	6.556

20	Costunolide	$C_{15}H_{20}O_2$	1891	-	8.874
21	Dehydrocostus lactone	$C_{15}H_{18}O_2$	1962	-	55.399
22	Unknown	-	2118	-	0.446
23	Unknown	-	2146	-	0.44
	Total				**82.75**
Sesquiterpene hydrocarbons: 5.94%; Sesquiterpene oxygenated: 75.92%; Unknown: 0.89					

3.2. Nanoparticles characterization

3.2.1. Dynamic light scattering measurements

According to **Table 2**, the average size (Z-average) of the PMMA-NP entrapped with SL-EO was significantly higher than that of blank NP ($p < 0.05$). Similar results were already reported in the literature (Lammari et al., 2020a; Rosset et al., 2012). Jummes et al. (2020) noticed larger sizes for palmarosa EO loaded poly-ε-caprolactone NP compared to the unloaded NP. They related the smallest particle size of empty NP to their empty interior. With respect to the PDI, low values were shown in this study (less than 0.2) with no significant ($p > 0.05$) difference between free and loaded-NP. Apparently, the PDI value reflected the aggregation level of NP (Jummes et al., 2020); thus, in the current study, the low PDI value reflected an homogeneous distribution of all particles.

The ζ-potential represents the overall surface charge that a particle acquires in a particular medium and it serves as a key indicator of the dispersion stability. Particles exhibiting ζ-potential values greater than +30mV or less than −30mV are colloidally stable due to repulsive electrostatic interactions (Barhoum et al., 2018). In this study, PMMA-NP exhibited a good colloidal stability since no aggregation has been observed and confirmed by the measured ζ-potential values ranging from +39 to +45 mV for free and loaded-NP, respectively. The positive charge of PMMA-NP was attributed to the ammonium

quaternary groups of the polymer as previously described (Froiio et al., 2019). Higher ζ-potential values were found for SL-EO loaded-NP as compared to free NP due to the interaction of the EO with PMMA polymer. This result was in accordance with our previous study when encapsulating *Phoenix dactilyfera* seeds oil (Lammari et al., 2020a).

Table 2. Particle size, polydispersity index and ζ-potential of blank and loaded PMMA nanoparticles.

	Z-average (nm)	**PDI**	**ζ-potential (mV)**
Blank NP	45 ± 2	0.19 ± 0.01	+39 ± 2
Saussurea lappa EO loaded-NP	145 ± 1	0.18 ± 0.01	+45 ± 2

3.2.2. Nanoparticle morphology

Morphological characterization of the NP containing SL-EO by transmission electron microscopy showed that the NP exhibited spherical and regular form, as depicted in **Fig. 2.**

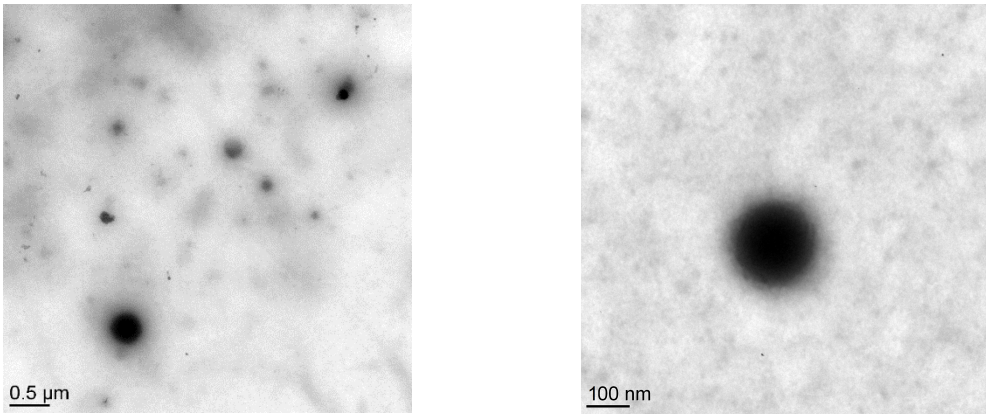

Fig. 2. Transmission Electron Microscopy images of *Saussurea lappa* EO loaded PMMA nanoparticles at 0.5 and 0.1 µm scale bar.

3.2.3. Fourier transform infrared spectroscopy analysis

Fourier transform infrared spectroscopy analysis was carried out to investigate the chemical interaction between SL-EO and PMMA. Apparently, drug-polymer interaction

resulted in changes in FTIR spectra (Yenilmez, 2017). The FTIR patterns of SL-EO, PMMA and loaded-NP were shown in **Fig. 3**. In PMMA spectrum, the peak at 2950 corresponded to the stretching vibration of C-H aliphatic groups. The peaks at 1722 cm^{-1} and 1143 cm^{-1} were assigned to the stretching vibrations of C=O and C-O ester group, respectively; while the band at 1446 cm^{-1} referred to the bending vibration of C-H aliphatic groups. This was in agreement with what was reported in the literature (Khurshid et al., 2016; Sibokoza et al., 2018). In SL-EO spectrum, the broad band at 3419 cm^{-1} was correlated to O–H group of α-elemol, β-eudesmol, α- and β-costol. The small peaks at 2925 and 1439 cm^{-1} were due to C–H symmetrical stretching and bending vibrations of saturated hydrocarbons, respectively (Riaz et al., 2018). The strong absorption band at 1762 cm^{-1} indicated a five membered lactone present in dehydrosaussurea lactone, dehydrocostus lactone and costunolide (Zaghloul et al., 2014). Band at 1640 cm^{-1} and those between 649 and 998 cm^{-1} were referred to the C=C stretching and bending of alkene, respectively, present in all the EO constituents.

The superposition of SL-EO and PMMA FTIR spectrums on that of EO loaded-nanoparticles revealed an increase in the peak intensity in 1724 cm^{-1} as well as coming out of peaks in 2927, 2856, 1764 and 650 cm^{-1} which characterized SL-EO. This might be attributed to the interaction between SL-EO and PMMA in the nanoparticles. Therefore, SL-EO was efficiently encapsulated within the polymeric nanoparticles.

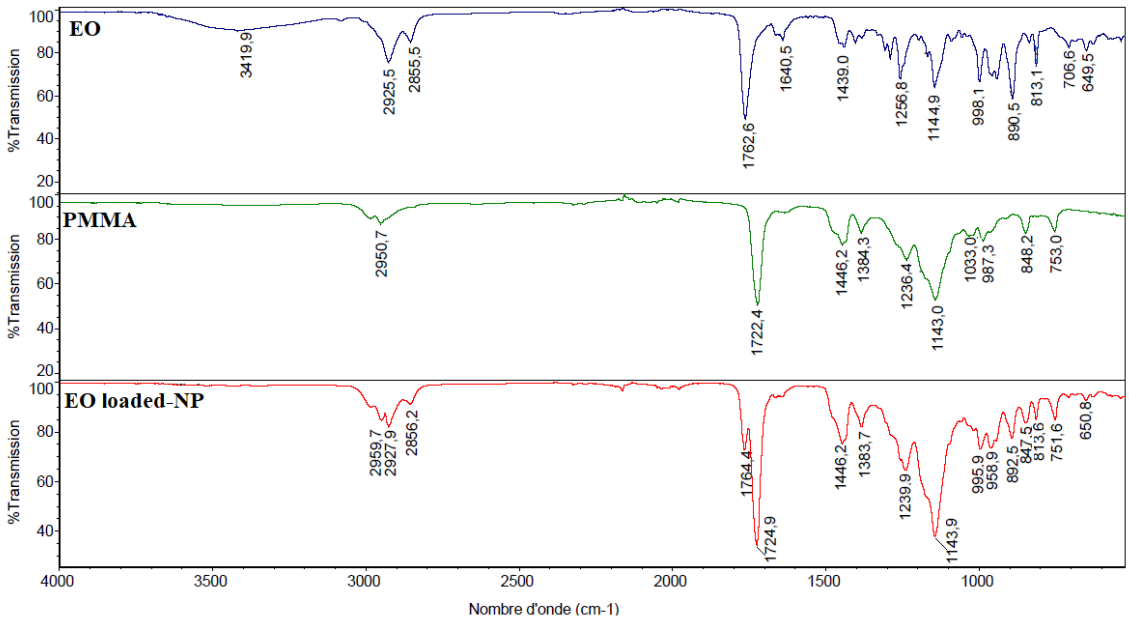

Fig. 3. Fourier transformed infrared spectroscopy (FTIR) spectrum noted between 650 cm^{-1} and 4000 cm^{-1} for unencapsulated *Saussurea lappa* EO, PMMA and EO loaded-Nanoparticles.

3.3. Stability study

The colloidal stability of SL-EO loaded-NP formulation was investigated by analyzing the size and the ζ-potential as a function of temperature (4°C, RT and 40°C) during one month. As demonstrated in **Fig.4A**, the average diameter of the prepared PMMA loaded-NP throughout the period of stability study was not changed significantly (ranging size was from 140 to 148 nm). The ζ-potential was found to be almost constant and in the vicinity of 45 mV +/- 5 mV at pH 6.

Moreover, the ζ-potential values of these NPs have been determined under different pH to get an idea about their stability upon biological applications. In this context, the ζ-potential was determined after the addition of either diluted HCl or NaOH to have different pH (3, 4, 5, 7, 9, 10 and 12) and the results are shown in **Fig.4B.** By increasing the pH from 3 to 12, the ζ-potential decreased from 45 to 32 mV. These results were in conformity with

those obtained by Du and coworkers (2004) for carboxymethyl konjac glucomannan–chitosan based-NP. In another study, the change in the ζ-potential measurements was related to the decrease of the charge density of the chitosan induced by the reduction of the concentration of H^+ ions (Boddohi et al., 2008). Although the ζ-potential decreased by varying pH, the NP remained stable with a ζ-potential around +32 mV.

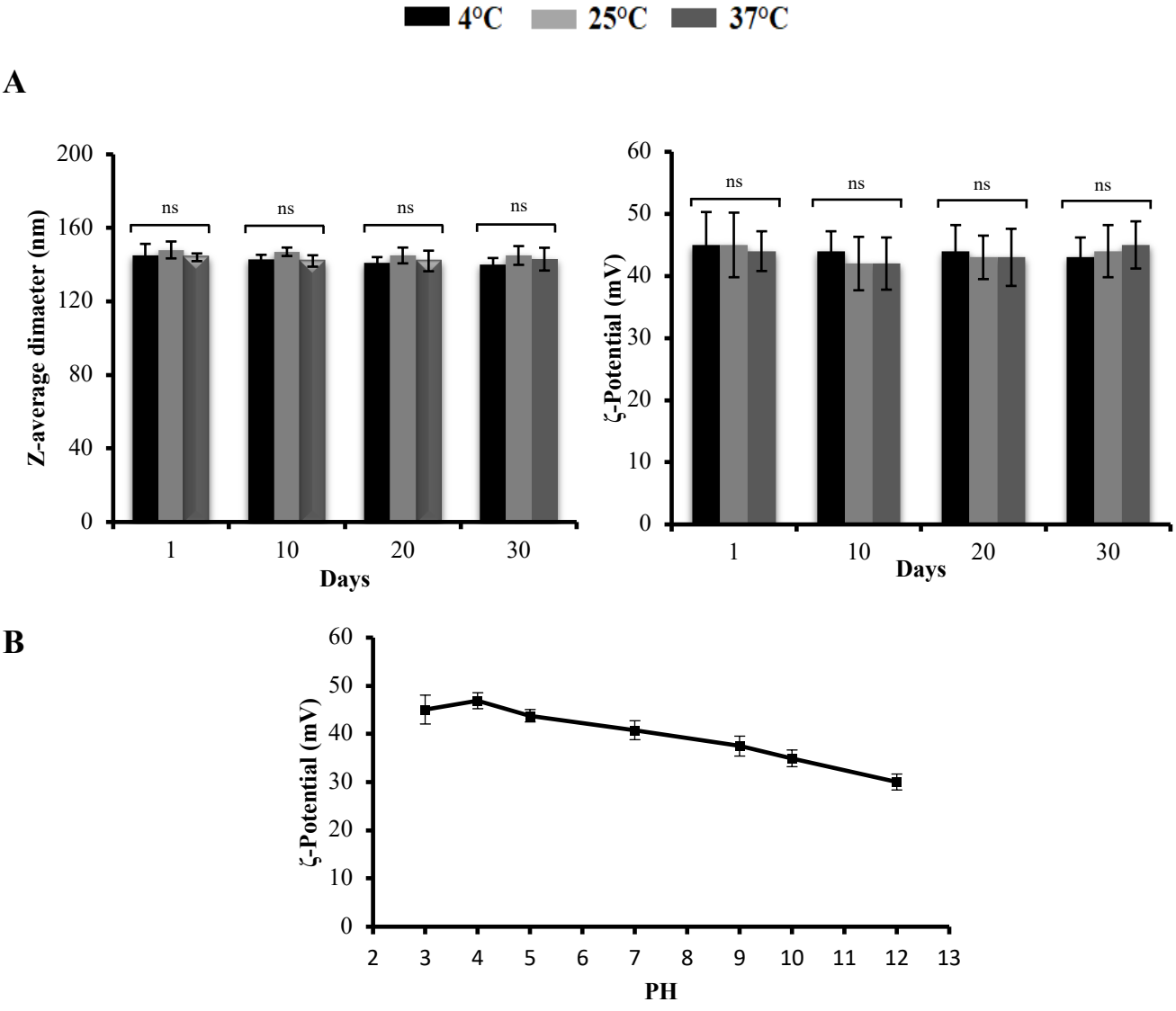

Fig. 4. Stability of PMMA based nanoparticles containing *Saussurea lappa* EO in terms of size, ζ-potential (A) and pH (B). Measurements from separate tests were combined (n = 3) and represented as mean ± SD; ns indicates not significant difference (p-value > 0.05).

3.4. *In vitro* cytotoxicity

The human lung epithelial A549 cell line is derived from an alveolar adenocarcinoma and has an epithelial like-morphology and is commonly used as *in vitro* model for cytotoxicity screening of formulations (Carterson et al., 2005). In the current study, LDH cytotoxicity test was used to determine the cell viability. LDH test is an indirect and colorimetric method to check cellular cytotoxicity. It measures the concentration of LDH enzyme released from the damaged cells. Released LDH catalyzes lactate oxidation to pyruvate with simultaneous reduction of NAD^+ to $NADH/H^+$ that in turn reduces tetrazolium salt to a red colored formazan that can be detected by spectrophotometry. The quantity of formed color reflects the amount of released LDH and thus cell viability (Aslantürk, 2017).

In this study, A549 cells were first treated in a concentration-dependent manner with SL-EO loaded-NP formulations at different concentrations (12.5, 25, 50, 75, 100 and 200 µg/mL of oil content). Similarly, the effect of un-encapsulated SL-EO along with DMSO and blank NP on cell viability was investigated and the results are shown in **Fig.5**. The non-cytotoxicity of free NP confirms the biocompatibility of the used polymer. Several works reported no detectable cytotoxicity after PMMA-NP treatment on many cell lines including HaCaT (human keratinocyte), RAW264 (monocyte/macrophage-like cells), MDA-MB231 (invasive human breast adenocarcinoma), FaDu (pharynx carcinoma cells), MCF-7 (non-invasive human breast adenocarcinoma) (Gargouri et al., 2009), NR8383 macrophages (Eidi et al., 2010), CAM (chorioallantoic membrane) and rabbit corneal epithelial cell lines (Katzer et al., 2014). Moreover, SL-EO loaded-NP exhibit a dose-dependent cytotoxic effect. For instance, NP at higher concentrations (≥50 µg/mL) were

considered as cytotoxic whereas NP containing both 25 and 12.5 µg/mL were shown as non-cytotoxic. This result was in agreement with what Nayal et al. reported when they investigated the *in vitro* cytotoxicity of *Lippia dulcis* Trev. EO on Hep G2 cells (Nayal et al., 2009). They found that the EO reduced cells viability in a concentration and time-dependent manner. Similar results were also reported in the literature (Montero-Villegas et al., 2018). Moreover, the encapsulated -EO is more cytotoxic than its un-encapsulated form (especially at higher concentration) which can be attributed to the nanoencapsulation concept. As reported earlier, the nanoencapsulation may increase the cellular uptake and the bioavailability of essential oils as compared to their free form (Lammari et al., 2020b).

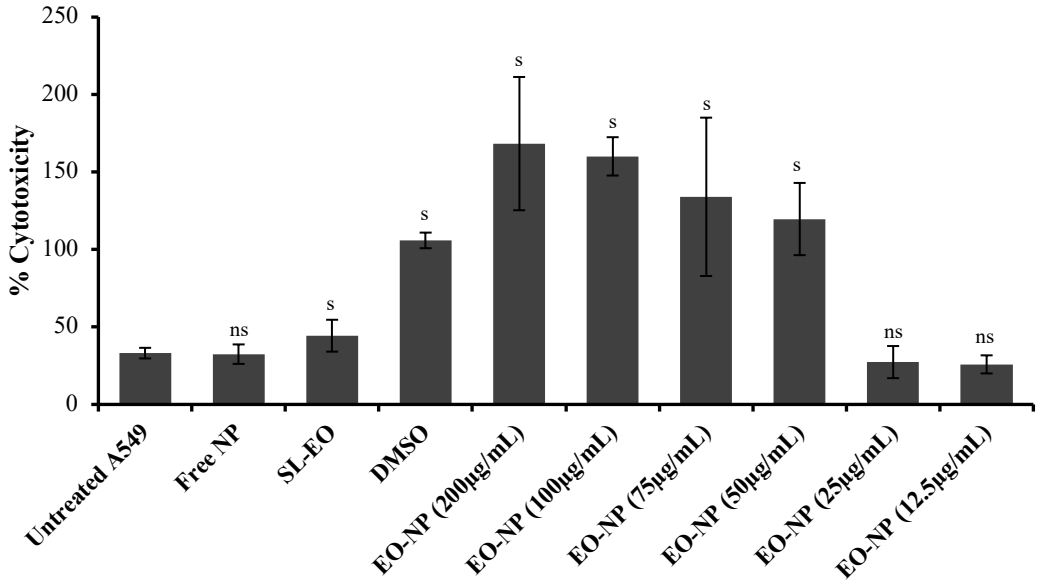

Fig.5. Cytotoxic effect of *Saussurea lappa* EO in its free and encapsulated form; s: significantly different from the control cells; ns: not significantly different from the control cells.

Interestingly, these findings corroborate cell morphologic changes. **Fig.6** shows micrographs of untreated and treated A549 cells. Light microscopic observation shows that

cells changed their morphology when cultured in the presence of SL-EO loaded-NP at concentrations more than 50 µg/mL (**Fig. 6. d, e** and **f**). Contrary in A549 control cells, structural alterations, reduction of A549 cell populations, and destruction of the cytoplasm could be observed. However, cells treated with SL-EO loaded-NP at 12.5 and 25µg/mL were similar to control cells where higher confluency, bigger nuclei and intact cytoplasm were visualized (**Fig.6. b** and **c**). This finding confirms the non-cytotoxicity of the developed nanoparticles at these two concentrations (12.5 and 25µg/mL).

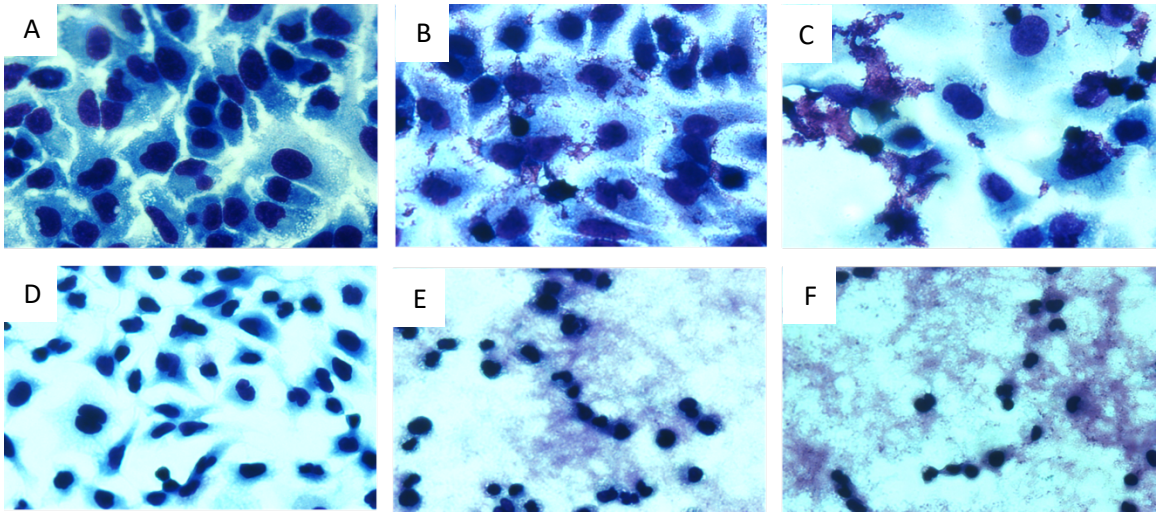

Fig.6. Representative micrographs of cell morphology after various treatments: a) Untreated cells; b) Cells treated with EO-loaded NP (12.5µg/mL); c) Cells treated with EO-loaded NP (25µg/mL); d) Cells treated with EO-loaded NP (75µg/mL); e) Cells treated with EO-loaded NP (100µg/mL) and f) Cells treated with EO-loaded NP (200µg/mL). Magnification x400.

3.6. Anti-inflammatory effect

Among the characteristic features of host inflammatory response to an insulting agent (e.g., bacteria, viruses, toxins) the production and release of pro-inflammatory mediators, including cytokines such as interleukin (IL)-1, IL-6 and IL-10 and tumor necrosis factor-alpha (TNF-α). This latter induces in turn the production of other inflammatory cytokines like granulocyte-macrophage colony-stimulating factor (GM-CSF) and potentiate the inflammation (Kany et al., 2019).

In addition to cytokines, increased production of matrix-degrading proteases has been associated with inflammation. These include the matrix metalloproteinases (MMP) such as MMP-9 and MMP-2, a family of proteolytic enzymes involved in tissue remodeling (Shoshani et al., 2005) and inflammation modulation (Manicone and Mcguire, 2008). Literature survey revealed that both costus root extract and its main sesquiterpene lactones were widely studied for their anti-inflammatory effects; while, a formulation of such extract employing nanoparticles has never been studied for this context.

To address this aspect, A549 cells were incubated with SL-EO loaded nanoparticles (25µg/mL) for 1h prior to LPS treatment. This latter is known to trigger inflammatory-mediators expression and release by A549 cells. After the end of the treatments, mRNA expression of TNF-α, IL-1β and GM-CSF was investigated using RT-qPCR. The stimulation of A549 with LPS resulted in a strong increase of mRNA expression of the inflammatory factors (**Fig.7)**. Similar results were obtained with free nanoparticles treatment (without EO) especially for TNF-α and GM-CSF. Interestingly, a high reduction of all the cytokines was observed upon treatment with SL-EO loaded-NP (**Fig.7**) suggesting strongly the anti-inflammatory effect mediated by SL-EO. Both dehydrocostuslactone and costunolide were reported as potential inhibitors of the

expression of TNF-α (Choodej et al., 2018; Seo et al., 2015)(Rayan et al., 2011) and IL-1β (Kang et al., 2004; Rayan et al., 2011)(He et al., 2019). The activity of these two constituents was not limited on these two cytokines. In a recent study carried by Zhou et al. (Zhou et al., 2020), dehydrocostus lactone extracted from the roots of SL reduced the expression of other inflammatory mediators like myeloperoxidase (MPO), superoxide dismutase (SOD), MCP-1, IL-17, IL-6 and IL-23, inflammatory signaling pathway (those associated with COX2, IL-6, IL-23, iNOS, GP130 and L-17), and colorectal mucosal barrier-related regulatory factors (XBP1s and MUC2). Subsequently, costunolide was shown to negatively regulates the expression of IL-6, MCP-1, Cox2, iNOS and NF-κB nuclear translocation in activated murine BV-2 microglia (Rayan et al., 2011). Li et al. related the biological effect of costunolide and dehydrocostus lactone to their α-methylene-γ-butyrolactone ring which is the key moiety of these two sesquiterpenes (Li et al., 2020). Further LDH cytotoxicity assay was used to determine the cell viability upon LPS treatment and results confirm the non-cytotoxicity of all the formulations (**Fig.8**).

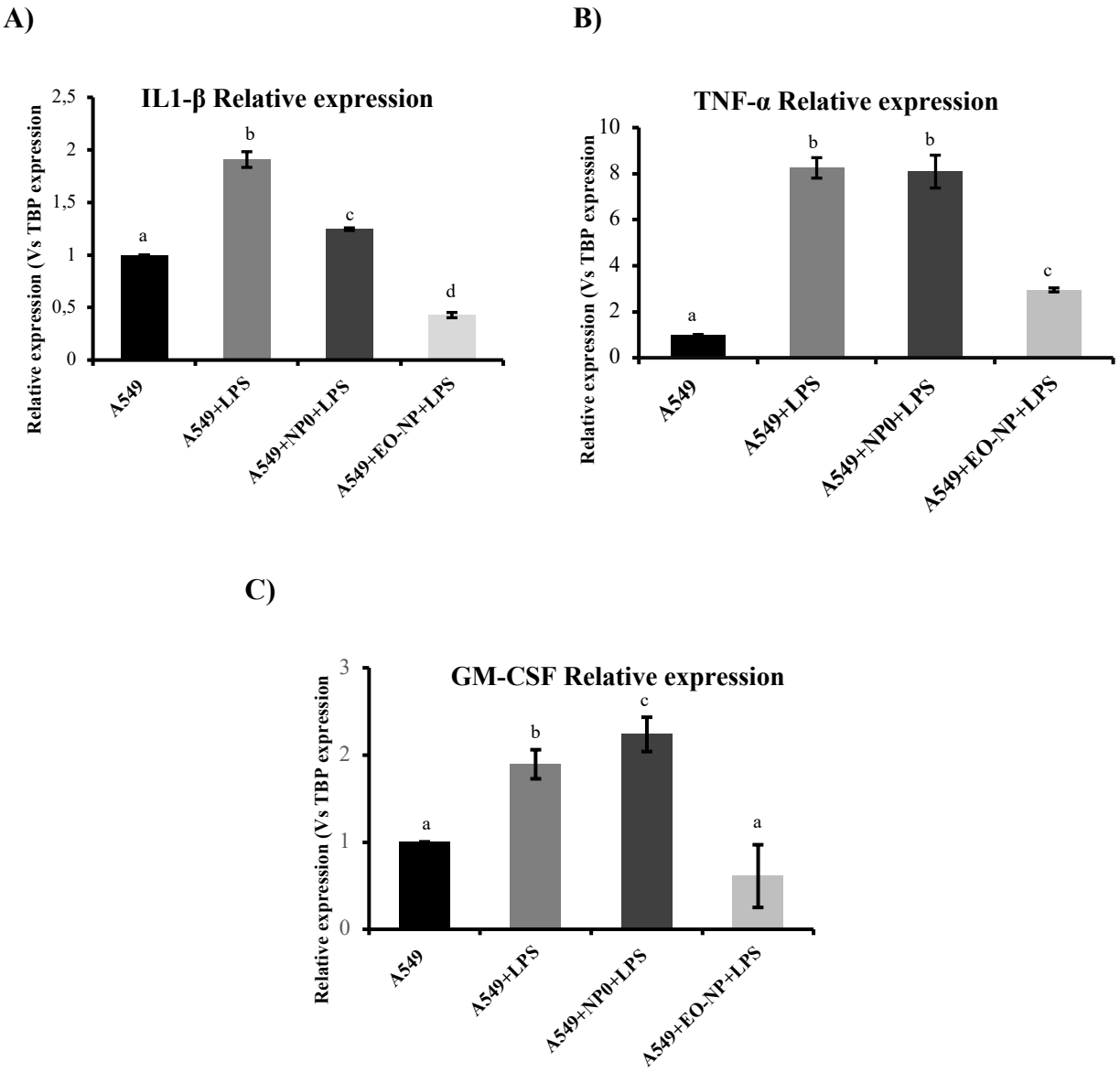

Fig.7. RNA expression of LPS-induced IL-1β **(A)**, TNF-α **(B)** and GM-CSF **(C)** after A549 treatment with free PMMA-based NP and SL-EO loaded PMMA-based NP 25 µg/mL. Measurements from independent wells and reproducible, represented as mean ± SD. Different letters indicate significant difference (p-value < 0.05).

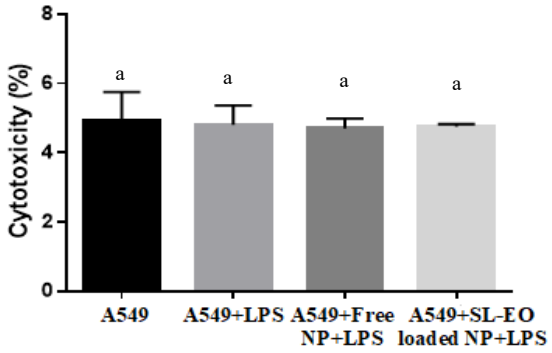

Fig.8. Cytotoxic effect of *Saussurea lappa* EO in its free and encapsulated form (25µg/mL) upon LPS stimulation. Different letters indicate significant difference (p-value < 0.05).

Furthermore, a gelatin zymography was performed to assess the level of MMP in the medium released from all the treated A549 cells and the results are reported in **Fig. 9**. In this study, we focused on MMP-9. MMP-9 is implicated in the degradation of gelatin and collagen type IV, major components of the basement membrane and extracellular matrix (Kim et al., 2012). It is also of particular interest for inflammation because of its role in neutrophil infiltration and cytokine cleavage (Bradley et al., 2012; Sorokin, 2010). Our data show that LPS stimulates MMP-9 enzyme production, while a reduction was noticed after SL-EO loaded-NP treatment (**Fig.9**). This results was in accordance with previous work studies where both costunolide (He et al., 2019) and dihydrocostus lactone (Kim et al., 2012) exhibited remarkable inhibition of MMP-9. Altogether, our data demonstrate that SL-EO possesses anti-inflammatory properties.

A)

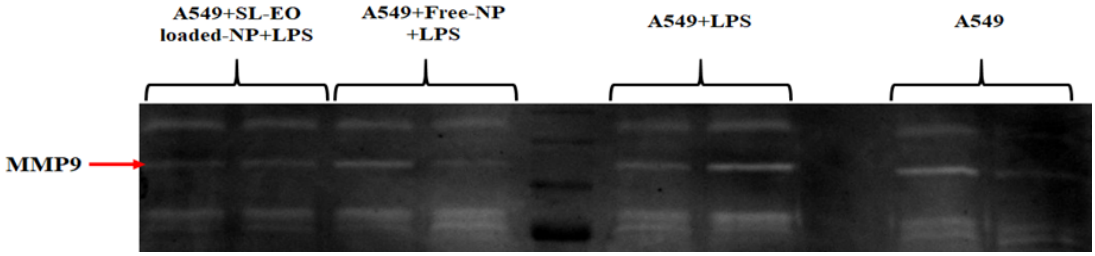

B)

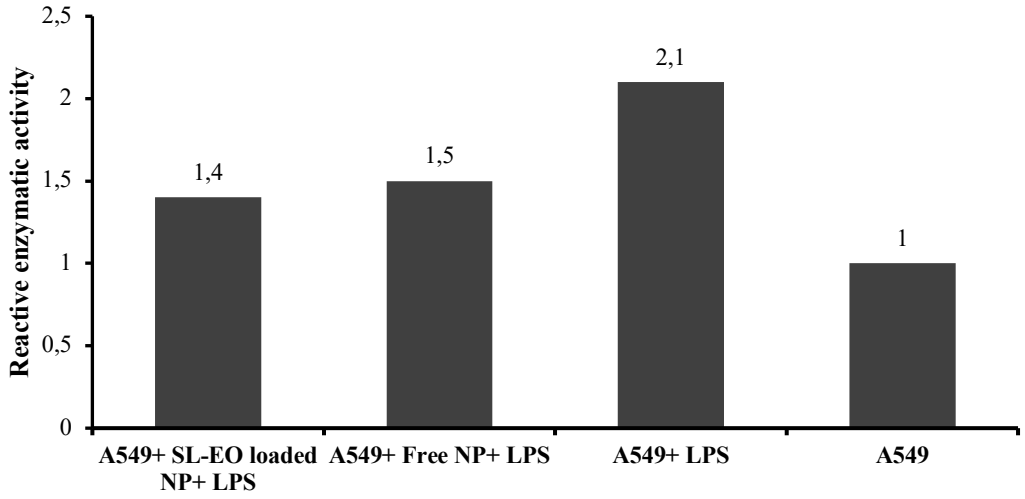

Fig.9. Gelatin zymography for MMP9 (A) and densitometry (B) after A549 treatment with free PMMA-based NP and SL-EO loaded PMMA-based NP 25 µg/mL.

3.8. *In vitro* anticholinesterase activity

Alzheimer's disease is among the major global public health priority and recently its prevalence has been increasing at an alarming rate. It is a chronic neurodegenerative disorder of the brain characterized by progressive decline of activities of daily living, behavior, and cognition. Alzheimer's disease is secondary to deficits in central cholinergic neurotransmission resulting from a loss of the neurotransmitter (acetylcholine) (Grossberg, 2003; Znati et al., 2020). Cholinesterase inhibitors seem to be a promising strategy to manage Alzheimer's disease by inhibiting the enzymes that degrade acetylcholine (i.e.

acetylcholinesterase and butyrylcholinesterase), thereby increasing the availability of acetylcholine to stimulate the receptors within the brain (Lane et al., 2005; Mesulam et al., 2002). In this study, we addressed for the first time the anticholinesterase activity of free SL-EO, unloaded-NP and SL-EO loaded-NP and compared it to that of the standard drug: Galantamine. The results are illustrated in **Fig.10.**

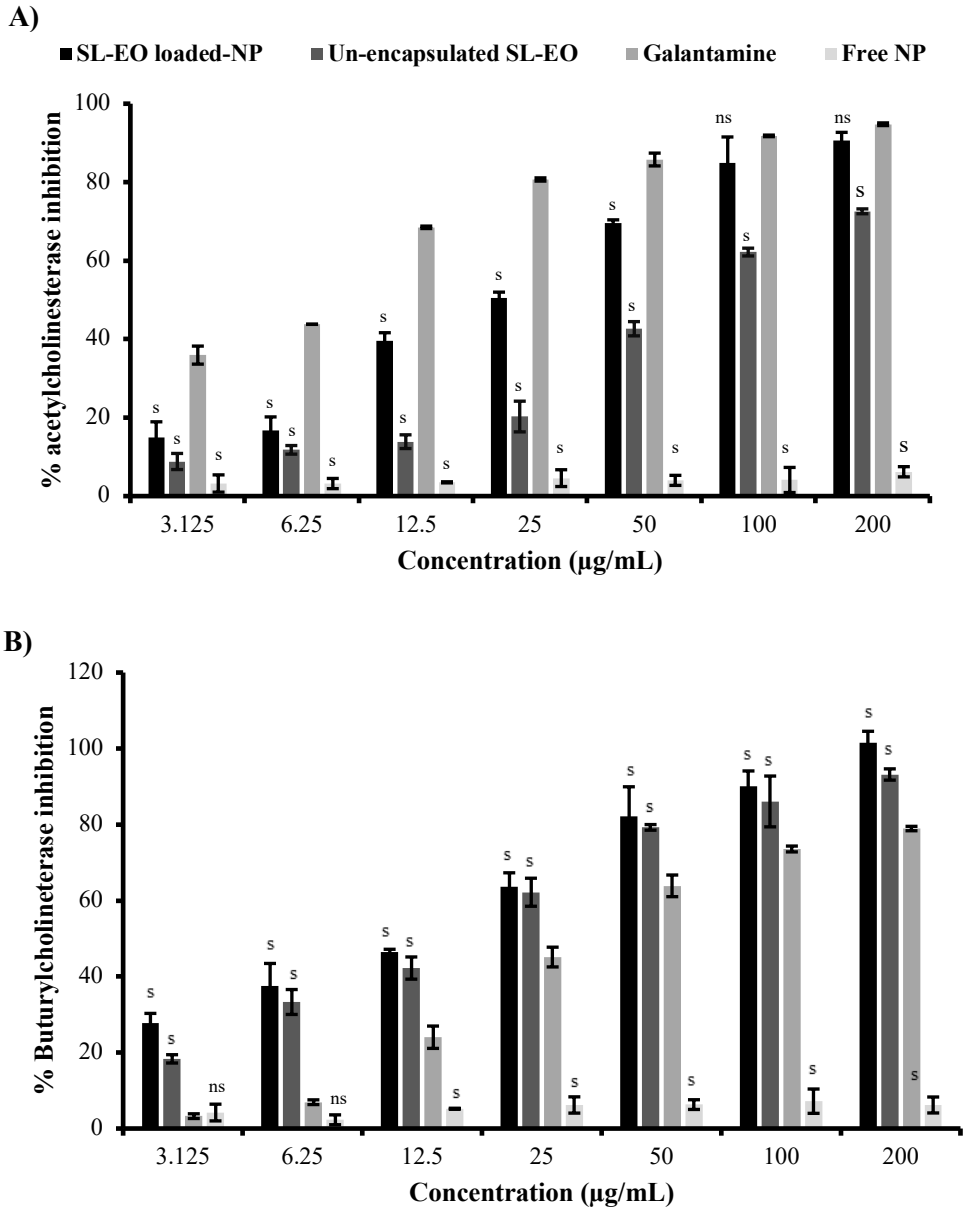

Fig.10. Acetylcholinesterase inhibition (A) and Butyrylcholinesterase inhibition (B) of unencapsulated SL-EO, free PMMA-based NP, SL-EO loaded PMMA-based NP and galantamine. Measurements from separate tests were combined (n = 3) and represented as mean ± SD; s: significantly different from the standard; ns: not significantly different from the standard.

All the tested samples inhibited acetylcholinesterase and butyrylcholinesterase activities *in vitro* in a dose dependent manner. Regarding butyrylcholinesterase, SL-EO loaded-NP showed an inhibition better than the standard drug: Galantamine. At the highest concentration (200 µg/mL), the ranked order of inhibition was as follow: SL-EO loaded-NP (101.6%) > un-encapsulated SL-EO (93.2%) > galantamine (78.9%), while with respect to acetylcholinesterase, the inhibition order at the highest concentration was as follow: galantamine (94.8%) > SL-EO loaded-NP (90.6%) > un-encapsulated SL-EO (72.6%). When comparing the inhibition of the unloaded-PMMA-NP (free-NP) with that of SL-EO loaded-NP against both enzymes, our data suggests that SL-EO exhibits an anti-Alzheimer property. This result was in agreement with a report by Ponnusankar and coworkers (2014) when they tested the *in vitro* acetyl- and butyrylcholinesterase inhibition of the methanolic extract of costus roots. Literature survey revealed also that sesquiterpene lactones have been previously reported as cholinesterase inhibitors (Hajimehdipoor et al., 2014; Hegazy et al., 2015; Ibrahim et al., 2013). Li et al. reported that the biological effect of costunolide and dehydrocostus lactone which are the main constituents of the SL-EO, is related to their α-methylene-γ-butyrolactone skeleton. For instance, the double bond of α-methylene-γ-butyrolactone produces an electrophilic entity capable of engaging in Michael-type reactions with nucleophilic groups of some essential groups of the active sites in the human body like amino acids or peptides (L-cysteine, glutathione) and enzymes

containing sulfhydryl groups (**Fig.11**) (Li et al., 2020; Padilla-Gonzalez et al., 2016). It was reported that the presence of free sulfhydryl groups in human cholinesterase enzymes molecules induced an irreversible inhibition in the micromolar range (Frasco et al., 2007). In the present study, the *in vitro* anti-Alzheimer activity was performed on horse serum-derived butyrylcholinesterase and *Electrophorus electricus*-derived acetylcholinesterase. The horse serum-derived butyrylcholinesterase showed 90.1% similarity with the human serum butyrylcholinesterase (Moorad et al., 1999), so it could be assumed that it contains sulfhydryl groups capable to react with the α-methylene-γ-butyrolactone of costunolide and dehydrocostus lactone. In support of this assumption, the high inhibitory effect of SL-EO against butyrylcholinesterase; the IC50 values were 17.4 ± 1.1 and 34.7 ± 2.0 µg/mL for un-encapsulated SL-EO and the standard drug, respectively, as illustrated in **Table 3.**

With respect to acetylcholinesterase, it was reported that free sulfhydryl groups were absent in *Electrophorus electricus* acetylcholinesterase and the enzyme inhibition occured in the millimolar range (Frasco et al., 2007). This explained the high IC50 value of SL-EO (67.4 ± 3.7 µg/mL) when compared to that against butyrylcholinesterase (IC50= 17.4 ± 1.1 µg/mL) or to that of standard drug (IC50= 6.3 ± 1.2 µg/mL).

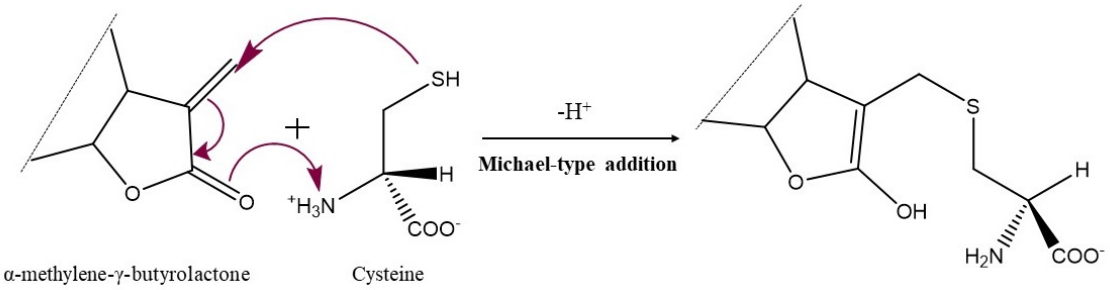

Fig.11. Mechanism of the Michael-type addition at α-methylene-γ-butyrolactone moiety of sesquiterpene lactones. The structure containing the sulfhydryl group (-SH) represents the nucleophile (protein cysteine residue, for example).

Fig.10 shows also that SL-EO in its encapsulated form showed better anti-cholinesterase activity than the un-encapsulated oil. A decrease in IC50 values was noticed for both enzymes, as depicted in **Table 3**. The IC50 values were 25.0 ± 2.0 and 67.4 ± 3.7 µg/mL against acetylcholinesterase; and 14.9 ± 8.0 and 17.4 ± 1.1 µg/mL against butyrylcholinesterase for SL-EO loaded-NP and un-encapsulated SL-EO, respectively. This was is accordance with previous reports where they asserted an enhancement in the biological activity upon EO encapsulation (Froiio et al., 2019)

It was reported earlier that the methanolic extract of the roots of SL inhibited acetyl- and butyrylcholinesterase with an IC50 equal to 58.68 ± 0.86 and 94.46 ± 0.5 μg/mL, respectively (Ponnusankar et al., 2014). These values were higher than those obtained in the present study. Thus, the developed NP may represent a promising formulation system for enhancing inhibition of Alzheimer-associated enzymes and potentially disease management. Of note, in addition to its lowest IC50 for both enzymes inhibition, the EO investigated in this study was extracted by a green process that provides credence to health claims and for quality assurance.

Table 3. IC50 of α-amylase, α-glucosidase, acetylcholinesterase and butyrylcholinesterase for unencapsulated SL-EO, SL-EO loaded PMMA-based NP and the reference compounds: Acarbose and Galantamine.

Sample	**IC50 (µg/mL)**			
	α-amylase	**α-glucosidase**	**AChE**	**BChE**
SL-EO	65.9 ± 1.7*	42.1 ± 3.0*	67.4 ± 3.7*	17.4 ± 1.1*
SL-EO loaded-NP	22.9 ± 0.3*	75.8 ± 4.4*	25.0 ± 2.0*	14.9 ± 8.0*
Acarbose	359.3 ±8.0	271.7 ± 7.1	-	-
Galantamine	-	-	6.3 ± 1.2	34.7 ± 2.0

IC50, is the concentration of samples required for 50% inhibition.

Each value is expressed as mean ± SD.

* Value is significantly different from the standard, acarbose or galantamine ($p < 0.005$).

AChE, Acetylcholinesterase; BChE, Butyrylcholinesterase.

3.9. *In vitro* α-amylase and α-glucosidase activity

Diabetes mellitus, a metabolic disorder characterized by hyperglycemia over a prolonged period of time, has emerged as an important cause of mortality and morbidity on a global scale. It is caused by either deficiency or impairment in the effectiveness of pancreatic insulin (Kharroubi and Darwish, 2015). One of the greatest challenges in diabetes management is the effective and consistent control of postprandial hyperglycemia. The healthy diet of diabetic people is an area of much debate. Currently, most experts agree that the total carbohydrate intake is a relatively reliable factor in predicting postprandial blood glucose (Sheard et al., 2004). The inhibition of α-amylase and α-glucosidase, enzymes involved in the digestion of carbohydrates, can significantly reduce the postprandial hyperglycemia (Agarwal and Gupta, 2016; Naquvi et al., 2011). In fact, α-amylase breaks down long chain carbohydrates; while α-glucosidase converts starch and disaccharides into simple sugar (glucose) (Nair et al., 2013). Therefore, the inhibition of these two enzymes seems to be an important strategy in the management of diabetes mellitus. In this context, the study of the antidiabetic effect of free SL-EO, unloaded-NP and SL-EO loaded-NP through inhibition of α-amylase and α-glucosidase was investigated, for the first time, *in vitro* and compared to that of standard drug: Acarbose. The results are shown in **Fig.12**.

All the samples inhibited α-amylase and α-glucosidase activities *in vitro* in a dose dependent manner. **Fig.12** shows that SL-EO exhibited inhibitory effect since the unloaded-PMMA-NP (free-NP) did not show any enzyme inhibition. This result confirms

the fact that costus species may reduce the blood glucose level. Raafat et al. reported that costus infrared extract has shown superiority in controlling gestational diabetes for pregnant groups with high safety profile on the offspring (Raafat et al., 2019). **Fig.12** reflects also that SL-EO showed better inhibition than the standard drug: acarbose against α-amylase and α-glucosidase. The IC50 values were 65.9 ± 1.7 and 359.3 ± 8.0 µg/mL against α-amylase; and 42.1 ± 3.0 and 271.7 ± 7.1 µg/mL against α-glucosidase for, un-encapsulated SL-EO and acarbose, respectively (**Table 3**). According to the literature, the antidiabetic effect of costus oil may be related to the presence of costunolide. Eliza et al. suggested that costunolide could effectively manage the glycemic control (Eliza et al., 2009). It was found that plasma glucose was significantly ($p< 0.05$) reduced in a dose-dependent manner upon costunolide administration to streptozotocin-induced diabetic rats when compared to the control. Additionally, the oral administration of costunolide (20mg/kg bw) significantly decreased glycosylated hemoglobin (HbA1c) and increased plasma insulin and tissue glycogen (Eliza et al., 2009). In a subsequent study, the increased sensitivity of insulin to uptake glucose by costunolide was ascribed to the stimulation of the beta islets to secrete insulin (Li et al., 2004). Regarding the chemical structure of diabetes controlling key enzymes, almost all α-glucosidases are reported to be highly inhibited by sulfhydryl-binding reagents (El-Shora et al., 2009; Faridmoayer and Scaman, 2005). This may explain the potent inhibitory activity of SL-EO against this enzyme. Alpha-amylases were also reported to possess sulfhydryl groups, but the inhibitory effect of SL-EO was not similar to that against α-glucosidase. It was noticed in an ancient work study that sulfhydryl groups were not absolutely required in α-amylase inhibition reaction since their complete oxidation coincided with 80% inactivation of the enzyme (Schramm,

1964). Padilla-Gonzalez et al. reported that the therapeutic effect of sesquiterpenes lactone did not restrict to the lactone moiety, although other structural moieties like epoxy, peroxy or aldehyde groups should not be ruled out (Padilla-Gonzalez et al., 2016).

In respect to α-amylase, SL-EO in its encapsulated form exhibited better inhibition when compared to the un-encapsulated form. IC50 values were 65.9 ± 1.7 and 22.9 ± 0.3 µg/mL for un-encapsulated SL-EO and SL-EO loaded-NP, respectively (**Table 3**). Similar results were reported earlier. *Psoralea corylifolia* extract loaded-NP exhibited better antidiabetic effect as compared to the free form (Shanker et al., 2017). Kavitha and coworkers (2017) related the enhancement in the antidiabetic activity of *Nilgirianthus ciliatus* NP to the sustained release property of these nanocarriers. On the other hand, unexpected results were shown with respect to α-glucosidase where SL-EO loaded-NP exhibited lower inhibition activity than the un-encapsulated form. The IC50 values were 42.1 ± 3.0 and 75.8 ± 4.4 for un-encapsulated SL-EO and SL-EO loaded-NP, respectively (**Table 3)**. This could be related to the fact that the oil needed more time to be released from PMMA-NP. In overall, SL-EO may be used as alternative for conditional oral hypoglycemic drugs in diabetes 2 managements known for their adverse effects like diarrhea, gastrointestinal discomfort, nausea, flatulence, cramping and weight gain (Fujisawa et al., 2005).

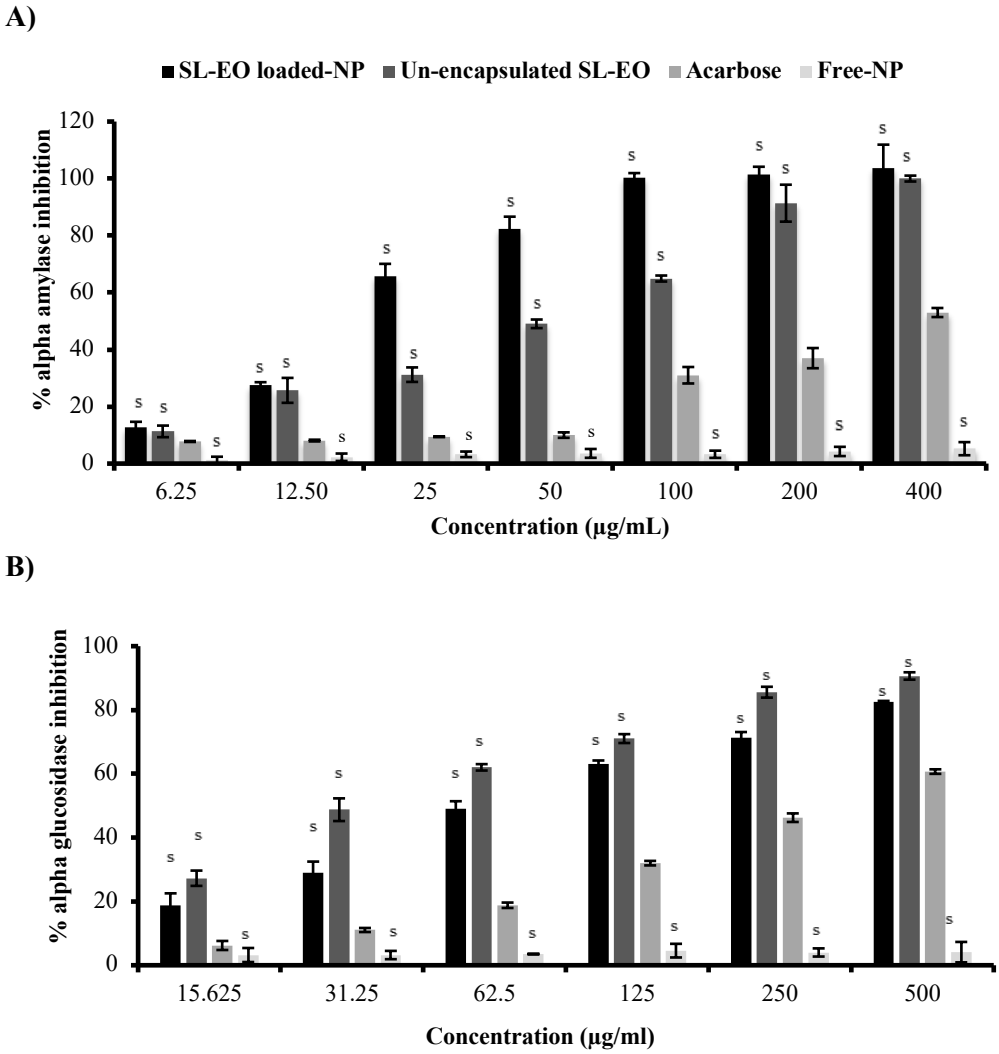

Fig.12. α-Amylase inhibition (A) and α-glucosidase inhibition (B) of unencapsulated SL-EO, free PMMA-based NP, SL-EO loaded PMMA-based NP and acarbose. Measurements from separate tests were combined (n = 3) and represented as mean ± SD; s: significantly different from the standard; ns: not significantly different from the standard.

4. Conclusion

Indeed the present study confirmed the important medicinal potential of *Saussurea lappa* CB. Clarke, known as costus, particularly with the extraction of its essential oil by means of supercritical fluid extraction, an innovative, clean, and environmetally friendly technique. Beneficial properties due to the anti-inflammatory, anti-Alzheimer and antidiabetic potentials of the extracted essential oil with dehydrocostus lactone (55.39 %) and costunolide (8.87%) as the major constituents, are reinforced by its encapsulation in PMMA based-NP of sizes order of 145 nm, a high ζ-potential value of +45 mV and a good stability upon one-month storage at different temperatures and pH. The *in vitro* cytotoxicity studies were performed on A549 cell lines and the loaded nanoparticles at 25 $\mu g \cdot mL^{-1}$ did not exhibit any cytotoxic effect and significant alterations on cells cytoplasm and nuclei were observed microscopically at higher essential oil concentration ($\geq$ 50 $\mu g.mL^{-1}$). The obtained results did also confirm the better efficiency of the designed nanoparticles in the treatment of diabetes type 2 than that of acarbose. The IC50 were equal to 22.9 and 75.8 $\mu g \cdot mL^{-1}$ against α-amylase and α-glucosidase, respectively. A high anti-Alzheimer's effect was noticed also with IC50 values around 25.0 and 14.9 $\mu g \cdot mL^{-1}$ against acetylcholinesterase and butyrylcholinesterase, respectively. The qRT-PCR and gelatin zymography experiments demonstrated a significant diminution of inflammatory cytokines gene expression (TNF-α, GM-CSF and IL1β) and matrix metalloprotease-9 activity in LPS-induced inflammatory A549 cell line. Moreover, evidence that α-amylase, α-glucosidase, acetyl- and butyrylcholinesterase inhibitory activities might be related to the α-methylene-γ-butyrolactone moiety of dehydrocostus lactone and costunolide of the studied essential oil was shown. To the best of our knowledge, this is the first report of the

in vitro α-amylase, α-glucosidase and anticholinesterase inhibitory effects of *Saussurea lappa* essential oil loaded nanoparticles along with their anti-inflammatory activity. Based on the reported enzymes inhibition activities and biologically metalloproteases and decreased expression of inflammatory cytokines, *Saussurea lappa* essential oil loaded nanoparticles could pave the way to the development of new bioactive formulations or dietary supplements for potential management of Alzheimer, diabetes or inflammatory diseases without or with insignificant adverse effects by comparison to those generally produced by conventional synthetic drugs. Further investigations are warranted including *in vivo* studies (e.g., preclinical), pharmacokinetic properties, bioavailability and the underlying associated metabolic pathways before any firm conclusions can be drawn on the efficacy of SL on the pharmacological activities reported in this study.

Declaration of Competing Interest

The authors declare that they have no known competing financial interests or personal relationships that could have appeared to influence the work reported in this paper.

Funding

This research did not receive any specific grant from funding agencies in the public, commercial, or not-for-profit sectors.

Reference

Aanouz, I., Belhassan, A., El-Khatabi, K., Lakhlifi, T., El-ldrissi, M., Bouachrine, M., 2020. Moroccan medicinal plants as inhibitors against SARS-CoV-2 main protease: Computational investigations. J. Biomol. Struct. Dyn. 1–9. https://doi.org/10.1080/07391102.2020.1758790

Abdelwahab, S.I., Taha, M.M.E., Alhazmi, H.A., Ahsan, W., Rehman, Z., Bratty, M. Al, Makeen, H., 2019. Phytochemical profiling of Costus (*Saussurea lappa* Clarke) root essential oil, and its antimicrobial and toxicological effects. Trop. J. Pharm. Res. 18,

2155–2160. https://doi.org/10.4314/tjpr.v18i10.22

Agarwal, P., Gupta, R., 2016. Alpha-amylase inhibition can treat diabetes mellitus. Res. Rev. J. Med. Heal. Sci. 5, 1–8.

Ansari, S., Siddiqui, M.A., Maaz, M., 2018. Hepatocurative effect of *Saussurea lappa* C.B Clarke and artemisia absinthium, linn in chronic hepatitis B. J. Young Pharm. 10, 354–357. https://doi.org/10.5530/jyp.2018.10.78

Aslantürk, Ö.S., 2017. *In Vitro* cytotoxicity and cell viability assays: Principles, advantages, and disadvantages, in: Larramendy, M.L., Soloneski, S. (Eds.), Genotoxicity - A Predictable Risk to Our Actual World. IntechOpen, Madrid, pp. 1–18.

Asokkumar, S., Naveenkumar, C., Raghunandhakumar, S., Kamaraj, S., Anandakumar, P., Jagan, S., Devaki, T., 2012. Antiproliferative and antioxidant potential of beta-ionone against benzo(a)pyrene-induced lung carcinogenesis in Swiss albino mice. Mol. Cell. Biochem. 363, 335–345.

Atanasov, A.G., Waltenberger, B., Pferschy-Wenzig, E.M., Linder, T., Wawrosch, C., Uhrin, P., Temml, V., Wang, L., Heiss, S.S.H., Rollinger, J.M., Schuster, D., Breuss, J.M., Bochkov, V., Mihovilovic, M.D., Kopp, B., Bauer, R., Dirsch, V.M., Stuppner, H., 2015. Discovery and resupply of pharmacologically active plant-derived natural products: A review. Biotechnol. Adv. 33, 1582–1614.

Azeez, L., Lateef, A., Ayoade, L., Joshua, T., Rasheed, O., Mustapha, Z., 2020. Adsorption behaviour of rhodamine B on hen feather and corn starch functionalized with green synthesized silver nanoparticles (AgNPs) mediated with cocoa pods extracts. Chem. Africa 3, 237–250.

Barhoum, A., García-Betancourt, M.L., Rahier, H., Assche, G. Van, 2018. Physicochemical characterization of nanomaterials: polymorph, composition, wettability, and thermal stability, in: Barhoum, A., Makhlouf, A.S.H. (Eds.), Emerging Applications of Nanoparticles and Architecture Nanostructures. Elsevier Science Publishing Co Inc., New-York, pp. 255–278.

Bilia, A.R., Guccione, C., Isacchi, B., Righeschi, C., Firenzuoli, F., Bergonzi, M.C., 2014. Essential oils loaded in nanosystems : A developing strategy for a successful therapeutic approach. Evidence-Based Complement. Altern. Med. 2014, 1–14.

Boddohi, S., Killingsworth, C.E., Kippe, M.J., 2008. Polyelectrolyte multilayer assembly as a function of pH and ionic strength using the polysaccharides chitosan and heparin. Biomacromolecules 9, 2021–2028.

Bradley, L.M., Douglass, M.F., Chatterjee, D., Akira, S., Baaten, B.J.G., 2012. Matrix metalloprotease 9 mediates neutrophil migration into the airways in response to influenza virus-induced toll-like receptor signaling. PLoS Pathog. 8, e1002641. https://doi.org/10.1371/journal.ppat.1002641

Calixto, J.B., 2019. The role of natural products in modern drug discovery. An. Acad. Bras. Cienc. 91, 3. https://doi.org/0001-3765201920190105

Carterson, A.J., Bentrup, K.H. zu, Ott, M., Clarke, M.S., Pierson, D.L., Vanderburg, C.R., Buchanan, K.L., Nickerson, C.A., Schurr, M.J., 2005. A549 lung epithelial cells grown as three-dimensional aggregates: Alternative tissue culture model for Pseudomonas aeruginosa pathogenesis. Infect. Immun. 73, 1129–1140.

Chang, H.S., Lee, S.J., Yang, C.W., Chen, I.S., 2010. Cytotoxic sesquiterpenes from *Magnolia kachirachirai*. Chem. Biodivers. 7, 2737–2747. https://doi.org/10.1002/cbdv.200900418

Chavan, M.J., Wakte, P.S., Shinde, D.B., 2010. Analgesic and anti-inflammatory activity of Caryophyllene oxide from *Annona squamosa* L. bark. Phytomedicine 17, 149–151. https://doi.org/10.1016/j.phymed.2009.05.016

Chen, F., Tan, X., Tang, Q., Xing, X., 2011. GC-MS analysis of volatile oil from *Aucklandia lappa* from different producing areas. China Pharm. 22, 2187–2189.

Cheon, Y.H., Song, M.J., Kim, J.Y., Kwak, S.C., Park, J.H., Lee, C.H., Kim, J.J., Choi, M.K., Oh, J., Kim, Y.C., Yoon, K.H., Kwak, H.B., Lee, M.S., 2014. Costunolide inhibits osteoclast differentiation by suppressing c-Fos transcriptional activity. Phyther. Res. 28, 586–592. https://doi.org/10.1002/ptr.5034

Chifiriuc, M.C., Kamerzan, C., Lazar, V., 2017. Essential oils and nanoparticles: New strategy to prevent microbial biofilms, in: Ficai, A., Grumezescu, A.M. (Eds.), Nanostructures for Antimicrobial Therapy, first ed. Elsevier Science Publishing Co Inc., New-York, pp. 279–291.

Choodej, S., Pudhom, K., Mitsunaga, T., 2018. Inhibition of TNF-α-induced inflammation by sesquiterpene lactones from *Saussurea lappa* and semi-synthetic analogues. Planta Med. 84, 329–335. https://doi.org/10.1055/s-0043-120115

Contri, R. V., Ribeiro, K.L.F., Fiel, L.A., Pohlmann, A.R., Guterres, S.S., 2013. Vegetable oils as core of cationic polymeric nanocapsules: Influence on the physicochemical properties. J. Exp. Nanosci. 8, 913–924. https://doi.org/10.1080/17458080.2011.620019

Contri, R. V, Kulkamp-guerreiro, I.C., Janine, S., Frank, L.A., Pohlmann, A.R., Guterres, S.S., 2016. Nanoencapsulation of Rose-Hip oil prevents oil oxidation and allows obtainment of gel and film topical formulations. AAPS PharmSciTech 17, 863–871. https://doi.org/10.1208/s12249-015-0379-9

David, B., Wolfender, J.-L., Dias, D.A., 2015. The pharmaceutical industry and natural products: historical status and new trends. Phytochem. Rev. 14, 299–315.

Dhar, A., Maurya, S., Mishra, A., Singh, G., Singh, M., Seth, A., 2016. Preliminary screening of a classical Ayurvedic formulation for anticonvulsant activity. Anc. Sci. Life 36, 28. https://doi.org/10.4103/0257-7941.195410

Dillen, K., Bridts, C., Veken, P. Van der, Cos, P., Vandervoort, J., Augustyns, K., Stevens, W., Ludwig, A., 2008. Adhesion of PLGA or Eudragit®/PLGA nanoparticles to Staphylococcus and Pseudomonas. Int. J. Pharm. 349, 234–240.

Du, J., Sun, R., Zhang, S., Govender, T., Zhang, L., Xiong, C., Peng, Y., 2004. Novel polyelectrolyte carboxymethyl konjac glucomannan–chitosan nanoparticles for drug delivery. Macromol. rapid comminication 25, 954–958. https://doi.org/10.1002/marc.200300314

Eidi, H., Joubert, O., Attik, G., Duval, R.., Bottin, M.., Hamouia, A., Maincent, P., Rihn,

B.., 2010. Cytotoxicity assessment of heparin nanoparticles in NR8383 macrophages. Int. J. Pharm. 396, 156–65.

El-Asbahani, A., Miladi, K., Addi, H., Bitar, A., Casabianca, H., Abdelhamid, E.M., Hartmann, D., Jilale, A., Renaud, F., Elaissari, A., 2015. Antimicrobial activity of nano-encapsulated essential oils: comparison to non-encapsulated essential oils. J. Colloid Sci. Biotechnol. 4, 39–48.

El-Shora, H.M., Metwally, M.A., Khlaf, S.A., 2009. Essential groups and stability of α-glucosidase of *Penicillium notatum*. Ann. Microbiol. 59, 285–291.

Eliza, J., Daisy, P., Ignacimuthu, S., Duraipandiyan, V., 2009. Normo-glycemic and hypolipidemic effect of costunolide isolated from *Costus speciosus* (Koen ex. Retz.)Sm. in streptozotocin-induced diabetic rats. Chem. Biol. Interact. 179, 329–334. https://doi.org/10.1016/j.cbi.2008.10.017

Ellman, G.., Courtney, K.., Andres, V., Featherston, R.., 1961. A new and rapid colorimetric determination of acetylcholinesterase activity. Biochem. Pharmacol. 7, 88–95.

Faridmoayer, A., Scaman, C.H., 2005. Binding residues and catalytic domain of soluble *Saccharomyces cerevisiae* processing alpha-glucosidase I. Glycobiology 15, 1341–1348. https://doi.org/10.1093/glycob/cwj009

Fessi, H., Puisieux, F., Devissaguet, J.P., Ammoury, N., Benita, S., 1989. Nanocapsule formation by interfacial polymer deposition following solvent displacement. Int. J. Pharm. 55, R1–R4.

Frasco, M.F., Colletier, J.P., Weik, M., Carvalho, F., Guilhermino, L., Stojan, J., Fournier, D., 2007. Mechanisms of cholinesterase inhibition by inorganic mercury. FEBS J. 274, 1849–1861. https://doi.org/10.1111/j.1742-4658.2007.05732.x

Froiio, F., Ginot, L., Paolino, D., Lebaz, N., Bentaher, A., Fessi, H., Elaissari, A., 2019. Essential oils-loaded polymer particles: Preparation, characterization and antimicrobial property. Polymers (Basel). 11, 1017. https://doi.org/10.3390/polym11061017

Fujisawa, T., Ikegami, H., Inoue, K., Kawabata, Y., Ogihara, T., 2005. Effect of two α-glucosidase inhibitors, voglibose and acarbose, on postprandial hyperglycemia correlates with subjective abdominal symptoms. Metabolism 54, 387–390. https://doi.org/10.1016/j.metabol.2004.10.004

Gargouri, M., Sapin, A., Bouli, S., Becuwe, P., Merlin, J., Maincent, P., 2009. Optimization of a new non-viral vector for transfection: Eudragit nanoparticles for the delivery of a DNA plasmid. Technol. Cancer Res. Treat. 8, 433–444.

Gautam, H., Asrani, R.K., 2018. Phytochemical and pharmacological review of an ethno medicinal plant : *Saussurea Lappa.* Vet. Res. Int. 6, 1–9.

Giaretta, M., Bianchin, M.D., Kanis, L.A., Contri, R.V., Külkamp-Guerreiro, I.C., 2019. Development of innovative polymer-based matricial nanostructures for Ritonavir oral administration. J. Nanomater. 2019, 1–10. https://doi.org/10.1155/2019/8619819

Grossberg, G.T., 2003. Cholinesterase inhibitors for the treatment of Alzheimer's disease. Curr. Ther. Res. 64, 216–235. https://doi.org/10.1016/S0011-393X(03)00059-6

Hajimehdipoor, H., Mossadegh, M., Naghibi, F., Haeri, A., Hamzeloo-Moghadam, M., 2014. Natural sesquiterpene lactones as acetylcholinesterase inhibitors. An. Acad. Bras. Cienc. 86, 801–806. https://doi.org/10.1590/0001-3765201420130005

Hani, U., Sudeendra, R., Shivakumar, H.G., 2011. Formulation design and evaluation of Metronidazole microspheres in a bioadhesive gel for local therapy of vaginal candidiasis. Lat. Am. J. Pharm. 30, 161–167.

He, Y., Moqbel, S., Xu, L., Ran, J., Ma, C., Xu, K., Bao, J., Jiang, L., Chen, W., Xiong, Y., Wu, L., 2019. Costunolide inhibits matrix metalloproteinases expression and osteoarthritis via the NF-κB and Wnt/β-catenin signaling pathways. Mol. Med. Rep. 20, 312–322. https://doi.org/10.3892/mmr.2019.10239

Hegazy, M.-E., Ibrahim, A., Mohamed, T., Shahat, A., El Halawany, A., Abdel-Azim, N., Alsaid, M., Paré, P., 2015. Sesquiterpene lactones from *Cynara cornigera*: Acetyl cholinesterase inhibition and in silico ligand docking. Planta Med. 82, 138–146. https://doi.org/10.1055/s-0035-1558088

Herculano, E.D., Paula, H.C.B. De, Dias, F.G.B., Pereira, V.D.A., 2015. Physicochemical and antimicrobial properties of nanoencapsulated *Eucalyptus staigeriana* essential oil. LWT - Food Sci. Technol. 61, 484–491. https://doi.org/10.1016/j.lwt.2014.12.001

Huh, K.M., Lee, S.C., Cho, Y.W., Lee, J., Jeong, J.H., Park, K., 2005. Hydrotropic polymer micelle system for delivery of paclitaxel. J. Control. Release 101, 59–68. https://doi.org/10.1016/j.jconrel.2004.07.003

Ibrahim, M., Farooq, T., Hussain, N., Hussain, A., Gulzar, T., Hussain, I., Akash, M.S.H., Rehmani, F.S., 2013. Acetyl and butyryl cholinesterase inhibitory sesquiterpene lactones from Amberboa ramosa. Chem. Cent. J. 7, 116. https://doi.org/10.1186/1752-153X-7-116

Jummes, B., Sganzerla, W.G., da Rosa, C.G., Noronha, C.M., Nunes, M.R., Bertoldi, F.C., Barreto, P.L.M., 2020. Antioxidant and antimicrobial poly-ε-caprolactone nanoparticles loaded with *Cymbopogon martinii* essential oil. Biocatal. Agric. Biotechnol. 23, 101499. https://doi.org/10.1016/j.bcab.2020.101499

Kang, J.S., Yoon, Y.D., Lee, K.H., Park, S.K., Kim, H.M., 2004. Costunolide inhibits interleukin-1β expression by down-regulation of AP-1 and MAPK activity in LPS-stimulated RAW 264.7 cells. Biochem. Biophys. Res. Commun. 313, 171–177. https://doi.org/10.1016/j.bbrc.2003.11.109

Kany, S., Vollrath, J.T., Relja, B., 2019. Cytokines in inflammatory disease. Int. J. Mol. Sci. 20, 6008. https://doi.org/10.3390/ijms20236008

Katzer, T., Chaves, P., Bernardi, A., Pohlmann, A., Guterres, S., Beck, R.. R., 2014. Prednisolone-loaded nanocapsules as ocular drug delivery system: development, in vitro drug release and eye toxicity. J. Microencapsul. 31, 519–528.

Kaur, L., Singh, A., Kaur, J., 2019. A brief review of remedial uses of *Saussurea lappa*. J. Pharmacogn. Phytochem. 8, 4423–4430.

Kavitha, K., Sujatha, K., Manoharan, S., 2017. Biotherapeutic discovery development, characterization and antidiabetic potentials of *Nilgirianthus ciliatus* nees derived nanoparticles. J. Nanomed. Biother. Discov. 7, 152. https://doi.org/10.4172/2155-

983X.1000152

Kharroubi, A.T., Darwish, H.M., 2015. Diabetes mellitus: The epidemic of the century. World J. Diabetes 6, 850–867. https://doi.org/10.4239/wjd.v6.i6.850

Khurshid, M.F., Hussain, T., Masood, R., Hussain, N., 2016. Development and evaluation of a controlled drug delivery wound dressing based on polymeric porous microspheres. J. Ind. Text. 46, 986–999. https://doi.org/10.1177/1528083715612231

Kim, E.J., Hong, J.E., Lim, S.S., Kwon, G.T., Kim, J., Kim, J.S., Lee, K.W., Park, J.H.Y., 2012. The hexane extract of *Saussurea lappa* and its active principle, dehydrocostus lactone, inhibit prostate cancer cell migration. J. Med. Food 15, 24–32. https://doi.org/10.1089/jmf.2011.1735

Koparde, A., Doijad, R., Magdum, C., 2019. Natural products in drug discovery, in: Perveen, S., Al-Taweel, A. (Eds.), Pharmacognosy - Medicinal Plants. IntechOpen., Madrid, pp. 1–19.

Lammari, N., Froiio, F., Louaer, M., Cristiano, M.C., Bensouici, C., Paolino, D., Louaer, W., Meniai, A.H., Elaissari, A., 2020a. Poly (ethyl acrylate-co-methyl methacrylate-co-trimethylammoniethyl methacrylate chloride) (Eudragit RS 100) nanocapsules as nanovector carriers for *Phoenix dactylifera* L. seeds oil: a versatile antidiabetic agent. Biomacromolecules https://doi.org/10.1021/acs.biomac.0c00255

Lammari, N., Louaer, O., Meniai, A.H., Elaissari, A., 2020b. Encapsulation of essential oils via nanoprecipitation process : Overview, progress, challenges and prospects. Pharmaceutics 12, 431.

Lane, R.M., Potkin, S.G., Enz, A., 2005. Targeting acetylcholinesterase and butyrylcholinesterase in dementia. Int. J. Neuropsychopharmacol. 9, 101. https://doi.org/10.1017/S1461145705005833

Li, Q., Wang, Z., Xie, Y., Hu, H., 2020. Antitumor activity and mechanism of costunolide and dehydrocostus lactone: Two natural sesquiterpene lactones from the Asteraceae family. Biomed. Pharmacother. 125, 109955. https://doi.org/10.1016/j.biopha.2020.109955

Li, W.., Zheng, H.., Bukuru, J., De Kimpe, N., 2004. Natural medicines used in the traditional Chinese medical system for therapy of diabetes mellitus. J. Ethnopharmacol. 92, 1–21. https://doi.org/10.1016/j.jep.2003.12.031

Li, Z., Yuan, G., Lin, X., Liu, Q., Xu, J., Lian, Z., Song, F., Zheng, J., Xie, D., Chen, L., Wang, X., Feng, H., Zhou, M., Yao, G., 2019. Dehydrocostus lactone (DHC) suppresses estrogen deficiency-induced osteoporosis. Biochem. Pharmacol. 163, 279–289. https://doi.org/10.1016/j.bcp.2019.02.002

Lin, X., Peng, Z., Su, C., 2015. Potential anti-cancer activities and mechanisms of costunolide and dehydrocostuslactone. Int. J. Mol. Sci. 16, 10888–10906. https://doi.org/10.3390/ijms160510888

Liu, Z.L., He, Q., Chu, S.S., Wang, C.F., Du, S.S., Deng, Z.W., 2012. Essential oil composition and larvicidal activity of *Saussurea lappa* roots against the mosquito *Aedes albopictus* (Diptera: Culicidae). Parasitol. Res. 110, 2125–2130. https://doi.org/10.1007/s00436-011-2738-0

Lombardo, D., Kiselev, M.A., Caccamo, M.T., 2019. Smart nanoparticles for drug delivery application : Development of versatile nanocarrier platforms in biotechnology and nanomedicine. J. Nanomater. 2019, 1–26.

Ma, Q., Liang, T., Cao, L., Wang, L., 2018. Intelligent poly (vinyl alcohol)-chitosan nanoparticles-mulberry extracts films capable of monitoring pH variations. Int. J. Biol. Macromol. 108, 576–584. https://doi.org/10.1016/j.ijbiomac.2017.12.049

Ma, X., Williams, R.O., 2018. Polymeric nanomedicines for poorly soluble drugs in oral delivery systems: an update. J. Pharm. Investig. 48, 61–75.

Madhuri, K., Elango, K., Ponnusankar, S., 2012. *Saussurea lappa* (Kuth root): review of its traditional uses, phytochemistry and pharmacology. Orient. Pharm. Exp. Med. 12, 1–9.

Manicone, A., Mcguire, J., 2008. Matrix metalloproteinases as modulators of inflammation. Semin. Cell Dev. Biol. 19, 34–41. https://doi.org/10.1016/j.semcdb.2007.07.003

Matteucci, F., Giannantonio, R., Calabi, F., Agostiano, A., Gigli, G., Rossi, M., 2018. Deployment and exploitation of nanotechnology nanomaterials and nanomedicine, in: AIP Conference Proceedings. p. 0200001. https://doi.org/10.1063/1.5047755.

Mesulam, M., Guillozet, A., Shaw, P., Quinn, B., 2002. Widely spread butyrylcholinesterase can hydrolyze acetylcholine in the normal and alzheimer brain. Neurobiol. Dis. 9, 88–93. https://doi.org/10.1006/nbdi.2001.0462

Montero-Villegas, S., Crespo, R., Rodenak-Kladniew, B., Castro, M.A., Galle, M., Cicció, J.F., De-Bravo, M.G., Polo, M., 2018. Cytotoxic effects of essential oils from four *Lippia alba* chemotypes in human liver and lung cancer cell lines. J. Essent. Oil Res. 30, 167–181.

Moorad, D.R., Luo, C., Saxena, A., Doctor, B.P., Garcia, G.E., 1999. Purification and determination of the amino acid sequence of equine serum butyrylcholinesterase. Toxicol. Methods 9, 219–227. https://doi.org/10.1080/105172399242573

Mughees, M., Wajid, S., Samim, M., 2020. Cytotoxic potential of *Artemisia absinthium* extract loaded polymeric nanoparticles against breast cancer cells: Insight into the protein targets. Int. J. Pharm. 586, 119583. https://doi.org/10.1016/j.ijpharm.2020.119583

Na, B.R., Kim, H.R., Kwon, M.S., Lee, H.S., Piragyte, I., Choi, E.J., Choi, H.K., Han, W.C., Lee, S.H., Jun, C.D., 2013. Aplotaxene blocks T cell activation by modulation of protein kinase C-θ-dependent pathway. Food Chem. Toxicol. 62, 23–31. https://doi.org/10.1016/j.fct.2013.08.016

Nair, S.S., Kavrekar, V., Mishra, A., 2013. *In vitro* studies on alpha amylase and alpha glucosidase inhibitory activities of selected plant extracts. Eur. J. Exp. Biol. 3, 128–132.

Naquvi, K.J., Ahamad, J., Mir, S.R., Ali, M., Shuaib, M., 2011. Review on role of natural alpha-glucosidase inhibitors for management of diabetes mellitus. Int. J. Biomed. Res. 2, 374-380. https://doi.org/10.7439/ijbr.v2i6.121

Nayal, R., Abajy, M.Y., Melzig, M.F., 2009. Comparision of essential oil composition and

cytotoxicity of *Lippia dulcis* Trev. from Mexico and Panama. Int. J. Essent. Oil Ther. 3, 91–100.

Negi, J.S., Bisht, V.K., Bhandari, A.K., Kuniyal, C.P., Bhatt, V.P., Bisht, R., 2014. Chemical fingerprinting and antibacterial activity of *Saussurea lappa* clarke. Appl. Biochem. Microbiol. 50, 588–593.

Nguyen, L.T., Myslivečková, Z., Szotáková, B., Špičáková, A., Lněničková, K., Ambrož, M., Kubíček, V., Krasulová, K., Anzenbacher, P., Skálová, L., 2017. The inhibitory effects of β-caryophyllene, β-caryophyllene oxide and α-humulene on the activities of the main drug-metabolizing enzymes in rat and human liver *in vitro*. Chem. Biol. Interact. 278, 123–128. https://doi.org/10.1016/j.cbi.2017.10.021

Padilla-Gonzalez, G.F., dos Santos, F.A., Da Costa, F.B., 2016. Sesquiterpene lactones: More than protective plant compounds with high toxicity. CRC. Crit. Rev. Plant Sci. 35, 18–37. https://doi.org/10.1080/07352689.2016.1145956

Park, E.J., Park, S.W., Kim, H.J., Kwak, J.-H., Lee, D.-U., Chang, K.C., 2014. Dehydrocostuslactone inhibits LPS-induced inflammation by p38MAPK-dependent induction of hemeoxygenase-1 *in vitro* and improves survival of mice in CLP-induced sepsis *in vivo.* Int. Immunopharmacol. 22, 332–340. https://doi.org/10.1016/j.intimp.2014.07.012

Partheniadis, I., Zarafidou, E., Litinas, K.E., Nikolakakis, I., 2020. Enteric release essential oil prepared by co-spray drying methacrylate/polysaccharides—influence of starcht type. Pharmaceutics 12, 571. https://doi.org/10.3390/pharmaceutics12060571

Pattabhiramaiah, M., Rajarathinam, B., Shanthala, M., 2020. Nanoparticles and their application in folklore medicine as promising biotherapeutics, in: Prasad, D., Jeyabalan, T., Ram, S. (Eds.), Functional Bionanomaterials. Springer International Publishing., Berlin/Heidelberg, pp. 73–110.

Peng, Z., Wang, Y., Fan, J., Lin, X., Liu, C., Xu, Y., Ji, W., Yan, C., Su, C., 2017. Costunolide and dehydrocostuslactone combination treatment inhibit breast cancer by inducing cell cycle arrest and apoptosis through c-Myc/p53 and AKT/14-3-3 pathway.

Sci. Rep. 7, 41254.

Pina-Barrera, A.M., Alvarez-Roman, R., Baez-Gonzalez, J.G., Amaya-Guerra, C.A., Rivas-Morales, C., Gallardo-Rivera, C.T., Galindo-Rodriguez, S.A., 2019. Application of a multisystem coating based on polymeric nanocapsules containing essential oil of *Thymus vulgaris* L. to increase the shelf life of table grapes (*Vitis vinifera* L.). IEEE Trans. Nanobioscience 18, 549–557. https://doi.org/10.1109/TNB.2019.2941931

Ponnusankar, S., Elango, K., Kadiyala, M., 2014. Screening of siddha medicinal plants for its in-vitro acetylcholinesterase and butyrylcholinesterase inhibitory activity. Pharmacogn. Mag. 10, 294. https://doi.org/10.4103/0973-1296.133281

Raafat, K., El-Darra, N., Saleh, F., Rajha, H., Louka, N., 2019. Optimization of infrared-assisted extraction of bioactive lactones from *Saussurea lappa* L. and their effects against gestational diabetes. Pharmacogn. Mag. 15, 208–218. https://doi.org/10.4103/pm.pm_380_18

Rayan, N.A., Baby, N., Pitchai, D., Indraswari, F., Ling, E.A., Lu, J., Dheen, T., 2011. Costunolide inhibits proinflammatory cytokines and iNOS in activated murine BV2 microglia. Front. Biosci. 3, 1079–1091. https://doi.org/10.2741/e312

Riaz, M., Altaf, M., Faisal, A., Shekheli, M.A., Miana, G.A., Khan, M.Q., Shah, M.A., Ilyas, S.Z., Khan, A.A., 2018. Biogenic synthesis of AgNPs with *Saussurea lappa* C.B. Clarke and studies on their biochemical properties. J. Nanosci. Nanotechnol. 18, 8392–8398. https://doi.org/10.1166/jnn.2018.16414

Rosset, V., Ahmed, N., Zaanoun, I., Stella, B., Fessi, H., Elaissari, A., 2012. Elaboration of argan oil nanocapsules containing Naproxen for cosmetic and transdermal local application. J. colloid Sci. Biotechnol. 1, 218–224.

Sadik, I., Abd Allah, A., Abdulhameed, M., Abdelkader, M., Sayed, N., Nour, A., Algadir, A., 2017. Antioxidant activity and in-vitro potential inhibition of *Nigella sativa* and *Saussurea lappa* against LDL oxidation among sundance. E3 J. Med. Res. 6, 22–26. https://doi.org/10.18685/ejmr(6)3_ejmr-17-013

Scarponi, C., Butturini, E., Sestito, R., Madonna, S., Cavani, A., Mariotto, S., Albanesi, C., 2014. Inhibition of inflammatory and proliferative responses of human keratinocytes exposed to the sesquiterpene lactones dehydrocostuslactone and costunolide. PLoS One 9, e107904. https://doi.org/10.1371/journal.pone.0107904

Schramm, M., 1964. Unmasking of sulfhydryl groups in pancreatic α-amylase. Biochemistry 3, 1231–1234. https://doi.org/10.1021/bi00897a008

Seo, C.S., Lim, H.S., Jeong, S.J., Shin, H.K., 2015. Anti-allergic effects of sesquiterpene lactones from the root of *Aucklandia lappa* Decne. Mol. Med. Rep. 12, 7789–7795. https://doi.org/10.3892/mmr.2015.4342

Servat-Medina, L., González-Gómez, A., Reyes-Ortega, F., Sousa, I.M.O., Queiroz, N. de C.A., Zago, P.M.W., Jorge, M.P., Monteiro, K.M., Carvalho, J.E., San Román, J., Foglio, M.A., 2015. Chitosan-tripolyphosphate nanoparticles as *Arrabidaea chica* standardized extract carrier: synthesis, characterization, biocompatibility, and antiulcerogenic activity. Int. J. Nanomedicine 10, 3897–3909. https://doi.org/10.2147/IJN.S83705

Shanker, K., Mohan, G.K., Hussain, M.A., Jayarambabu, N., Pravallika, P.L., 2017. Green biosynthesis, characterization, *in vitro* antidiabetic activity, and investigational acute toxicity studies of some herbal-mediated silver nanoparticles on animal models. Pharmacogn. Mag. 13, 188–192.

Sheard, N.F., Clark, N.G., Brand-Miller, J.C., Franz, M.J., Pi-Sunyer, F.X., Mayer-Davis, E., Kulkarni, K., Geil, P., 2004. Dietary carbohydrate (amount and type) in the prevention and management of diabetes: a statement by the american diabetes association. Diabetes Care 27, 2266–2271. https://doi.org/10.2337/diacare.27.9.2266

Shoshani, Y., Pe'er, J., Doviner, V., Frucht-Pery, J., Solomon, A., 2005. Increased expression of inflammatory cytokines and matrix metalloproteinases in pseudophakic corneal edema. Investig. Opthalmology Vis. Sci. 46, 1940. https://doi.org/10.1167/iovs.04-1203

Sibokoza, S.B., Moloto, M.J., Mtunzi, F., Moloto, N., 2018. Diphenyldiselenide mediated

synthesis of copper selenide nanoparticles and their poly(methyl methacrylate) nanofibers. Asian J. Chem. 30, 1455–1459. https://doi.org/10.14233/ajchem.2018.21166

Singh, R., Chahal, K.K., Singla, N., 2017. Chemical composition and pharmacological activities of *Saussurea lappa* : A review. J. Pharmacogn. Phytochem. 6, 1298–1308.

Sonaje, K., Chen, Y.-J., Chen, H.-L., Wey, S.-P., Juang, J.-H., Nguyen, H.-N., Hsu, C.-W., Lin, K.-J., Sung, H.-W., 2010. Enteric-coated capsules filled with freeze-dried chitosan/poly(γ-glutamic acid) nanoparticles for oral insulin delivery. Biomaterials 31, 3384–3394. https://doi.org/10.1016/j.biomaterials.2010.01.042

Sorokin, L., 2010. The impact of the extracellular matrix on inflammation. Nat. Rev. Immunol. 10, 712–723. https://doi.org/10.1038/nri2852

Sousa, V.P. de, Crean, J., Borges, V.R. de A., Rodrigues, C.R., Tajber, L., Boylan, F., Cabral, L.M., 2013. Nanostructured systems containing babassu (*Orbignya speciosa*) oil as a potential alternative therapy for benign prostatic hyperplasia. Int. J. Nanomedicine 8, 3129–3139.

Sutar, N., Garai, R., Sharma, U.S., Singh, N., Roy, S.D., 2011. Antiulcerogenic activity of *Saussurea lappa* root. Int. J. Pharm. life Sci. 2, 516–520.

Tag, H.M., Khaled, H.E., Ismail, H.A.A., El-Shenawy, N.S., 2016. Evaluation of anti-inflammatory potential of the ethanolic extract of the *Saussurea lappa* root (costus) on adjuvant-induced monoarthritis in rats. J. Basic Clin. Physiol. Pharmacol. 27, 71–78. https://doi.org/10.1515/jbcpp-2015-0044

Tayel, S.A., El-Nabarawi, M.A., Tadros, M.I., Abd-Elsalam, W.H., 2013. Positively charged polymeric nanoparticle reservoirs of Terbinafine hydrochloride: Preclinical implications for controlled drug delivery in the aqueous humor of rabbits. AAPS PharmSciTech 14, 782–793.

Tian, X., Song, H.S., Cho, Y.M., Park, B., Song, Y.-J., Jang, S., Kang, S.C., 2017. Anticancer effect of *Saussurea lappa* extract via dual control of apoptosis and autophagy in prostate cancer cells. Medicine (Baltimore). 96, e7606.

https://doi.org/10.1097/MD.0000000000007606

Timbe, P.P.R., Motta, A. de S., Isaía, H.A., Brandelli, A., 2020. Polymeric nanoparticles loaded with *Baccharis dracunculifolia* DC essential oil: Preparation, characterization, and antibacterial activity in milk. J. Food Process. Preserv. 44. https://doi.org/10.1111/jfpp.14712

Umerska, A., Gaucher, C., Oyarzun-Ampuero, F., Fries-Raeth, I., Colin, F., Villamizar-Sarmiento, M., Maincent, P., Sapin-Minet, A., 2018. Polymeric nanoparticles for increasing oral bioavailability of curcumin. Antioxidants 7, 46. https://doi.org/10.3390/antiox7040046

Vadivelan, R., Krishnan, R.G., Kannan, R., 2019. Antidiabetic potential of Asparagus racemosus willd leaf extracts through inhibition of a-amylase and a-glucosidase. J. Tradit. Chinese Med. Sci. 9, 1–4. https://doi.org/10.1016/j.jtcme.2017.10.004

Veeresham, C., 2012. Natural products derived from plants as a source of drugs. J. Adv. Pharm. Technol. Res. 3, 200. https://doi.org/10.4103/2231-4040.104709

Yang, X., Huang, M., Jin, Y., Sun, L.-N., Song, Y., Chen, H.-S., 2012. Phenolics from *Bidens bipinnata* and their amylase inhibitory properties. Fitoterapia 83, 1169–1175. https://doi.org/10.1016/j.fitote.2012.07.005

Yenilmez, E., 2017. Desloratadine-Eudragit® RS100 nanoparticles: Formulation and characterization. Turkish J. Pharm. Sci. 14, 148–156. https://doi.org/10.4274/tjps.52523

Zaghloul, A.M., Yusufoglu, H.S., Salkini, M.A.A., Alam, A., 2014. New cytotoxic sesquiterpene lactones from *Anthemis scrobicularis.* J. Asian Nat. Prod. Res. 16, 922–929. https://doi.org/10.1080/10286020.2014.931377

Zahara, K., Tabassum, S., Sabir, S.S., Arshad, M., Qureshi, R., Amjad, M., Chaudhari, S., 2014. A review of therapeutic potential of *Saussurea lappa*-An endangered plant from Himalaya. Asian Pac. J. Trop. Biomed. 7, S60–S69.

Zheng, H., Chen, Y., Zhang, J., Wang, L., Jin, Z., Huang, H., Man, S., Gao, W., 2016. Evaluation of protective effects of costunolide and dehydrocostuslactone on ethanol-

induced gastric ulcer in mice based on multi-pathway regulation. Chem. Biol. Interact. 250, 68–77. https://doi.org/10.1016/j.cbi.2016.03.003

Zhou, Q., Zhang, W., He, Z., Wu, B., Shen, Z., Shang, H., Chen, T., Wang, Q., Chen, Y., Han, S., 2020. The possible anti-inflammatory effect of dehydrocostus lactone on DSS-induced colitis in mice. Evidence-Based Complement. Altern. Med. 2020, 1–8. https://doi.org/10.1155/2020/5659738

Znati, M., Zardi-Bergaoui, A., Daami-Remadi, M., Ben Jannet, H., 2020. Semi-synthesis, antibacterial, anticholinesterase activities, and drug likeness properties of new analogues of coumarins isolated from *Ferula lutea* (Poir.) Maire. Chem. Africa. https://doi.org/10.1007/s42250-020-00145-4